frontiers | Frontiers in Marine Science

TYPE Review
PUBLISHED 15 February 2023
DOI 10.3389/fmars.2023.1085618

OPEN ACCESS

EDITED BY
Rosie Chance,
University of York, United Kingdom

REVIEWED BY
Lucy J. Carpenter,
University of York, United Kingdom
Alex Baker,
University of East Anglia, United Kingdom

*CORRESPONDENCE
George W. Luther III
luther@udel.edu

SPECIALTY SECTION
This article was submitted to Marine Biogeochemistry, a section of the journal Frontiers in Marine Science

RECEIVED 31 October 2022
ACCEPTED 03 January 2023
PUBLISHED 15 February 2023

CITATION
Luther GW III (2023) Review on the physical chemistry of iodine transformations in the oceans. *Front. Mar. Sci.* 10:1085618. doi: 10.3389/fmars.2023.1085618

Review on the physical chemistry of iodine transformations in the oceans

George W. Luther III*

School of Marine Science and Policy, University of Delaware, Lewes, DE, United States

The transformation between iodate (IO_3^-), the thermodynamically stable form of iodine, and iodide (I^-), the kinetically stable form of iodine, has received much attention because these species are often dependent on the oxygen concentration, which ranges from saturation to non-detectable in the ocean. As suboxic conditions in the ocean's major oxygen minimum zones indicate that IO_3^- is minimal or non-detectable, the incorporation of IO_3^- into carbonate minerals has been used as a redox proxy to determine the O_2 state of the ocean. Here, I look at the one and two electron transfers between iodine species with a variety of oxidants and reductants to show thermodynamics of these transformations. The IO_3^- to IO_2^- conversion is shown to be the controlling step in the reduction reaction sequence due to thermodynamic considerations. As IO_3^- reduction to IO_2^- is more favorable than NO_3^- reduction to NO_2^- at oceanic pH values, there is no need for nitrate reductase for IO_3^- reduction as other reductants (e.g. Fe^{2+}, Mn^{2+}) and dissimilatory IO_3^- reduction by microbes during organic matter decomposition can affect the transformation. Unfortunately, there is a dearth of information on the kinetics of reductants with IO_3^-; thus, the thermodynamic calculations suggest avenues for research. Conversely, there is significant information on the kinetics of I^- oxidation with various oxygen species. In the environment, I^- oxidation is the controlling step for oxidation. The oxidants that can lead to IO_3^- are reactive oxygen species with O_3 and •OH being the most potent as well as sedimentary oxidized Mn, which occurs at lower pH than ocean waters. Recent work has shown that iodide oxidizing bacteria can also form IO_3^-. I^- oxidation is more facile at the sea surface microlayer and in the atmosphere due to O_3.

KEYWORDS

iodate, iodide, iodine intermediates, thermodynamics, oxidation, reduction

1 Introduction

The thermodynamically favorable form of iodine in seawater is iodate (IO_3^-). However, iodide (I^-) is present in oxic, suboxic and anoxic waters. The one electron transfer reaction of I^- with molecular oxygen, $^3O_2$, to form the iodine atom (I•) and superoxide (O_2^-) is thermodynamically unfavorable as is the reaction of two I^- with $^3O_2$ to form I_2 and H_2O_2 (Luther et al., 1995; Luther, 2011). Thus, other oxidants are required to initiate abiotic iodide oxidation, and I^- is a known sink for O_3. Biotic iodide oxidation has received much interest

with one report showing conversion of iodide to iodate (Hughes et al., 2021). Iodate reduction can occur with common reductants (e.g., sulfide, Fe^{2+}), and various organisms that decompose organic matter using iodate as the electron acceptor. Nitrate reductase and dimethyl sulfoxide reductase enzymes from these and planktonic microbes are considered important mediators for biotic iodate reduction (e.g., Hung et al., 2005; Amachi, 2008). Thus, there has been extensive interest in the chemistry of these two iodine species and the possible intermediates that form during their 6-electron redox interconversion ever since the element, iodine, was first discovered as I_2 during the study of brown kelp algae of the Laminariales (kelps/seaweeds) by Courtois in the early 1800s (Wong, 1991; Küpper et al., 2008; Küpper et al., 2011).

Possible chemical species that form during the $IO_3^- \leftrightarrow I^-$ interconversion are given in eqn. (1a, b). The loss of an O atom is equivalent to a two-electron transfer resulting in the reduction of the iodine from +5 in IO_3^- to +3 for IO_2^- (HOIO) to +1 for HOI (IO^-) and to -1 for I^-. The acid-base species in parentheses are minor species at seawater pH as the pK_a values for HOI and HOIO are 10.7 (K_a = 2 x 10^{-11}) and 4.49 (K_a = 3.2 x 10^{-5}), respectively.

$$IO_3^- \leftrightarrow IO_2^-(HOIO) \leftrightarrow HOI(IO^-) \leftrightarrow I^- \quad (1a)$$

Equation 1b shows the interconversion between HOI and I^- as HOI undergoes one-electron transfer to I_2 followed by another one-electron reduction per I atom to I^-.

$$HOI(IO^-) \leftrightarrow I_2 \leftrightarrow I^- \quad (1b)$$

This work considers the thermodynamics of these transformations during the reduction of IO_3^-, which occurs in anoxic systems, during organic matter decomposition and by phytoplankton, as well as the oxidation of I^-, which occurs by the direct oxidation of iodide by iodide oxidizing bacteria, oxidized metals and reactive oxygen species (ROS) that are produced by certain microbes, (macro)algae and abiotic processes including photochemistry. In a previous work (Luther, 2011), the chemistry and thermodynamics of chloride, bromide and iodide oxidation were compared; however, I(+3) species (HOIO, iodous acid, and IO_2^-, iodite) and stepwise iodate reduction were not considered. Here, stepwise reactions of the iodine species in equations 1a and 1b with environmentally important reactants (including transient ROS species) are considered for both the oxidation of I^- and the reduction of IO_3^- to affect their interconversion. The kinetics of these stepwise reactions are also considered. Kinetic data for the first step(s) in iodide oxidation are available, but less kinetic information is available for iodate reduction.

2 Methods

2.1 Calculations of aqueous redox potentials from half-reactions

Table 1 gives several equations for redox half-reactions that include the pH dependence for the reaction considered. These are pε(pH) relationships based on the balanced chemical equations and the thermodynamics of each chemical species. The basic mathematical approach has been fully developed in standard textbooks (Stumm and Morgan, 1996; Luther, 2016) and used in previous publications (Luther, 2010; Luther, 2011). Aqueous thermodynamic data to calculate the pε(pH) or logK(pH) relationships in Table 1 (at 25°C and 1 atm) are from Stumm and Morgan (1996) and other sources (Bard et al., 1985; Stanbury, 1989). The value used for the Gibbs free energy for Fe^{2+} (-90.53 kJ/mole) is that discussed in Rickard and Luther (2007). Values of the free energy for HOIO and IO_2^- are from Schmitz (2008).

The calculated pε value from each half-reaction is given as a function of pH as in the examples in Table 1, and these half reactions can be used for simple calculations of the pE values of full reactions (see next section). When H^+ or OH^- is not in a balanced equation for a half-reaction, there is no pH dependence on the half-reaction. The pε calculated is termed pε(pH) which provides a log K for each half-reaction at a given pH. Concentration dependence for the other reactants are not considered in the calculation; thus, these are considered standard state calculations. When concentration dependence is considered, the calculated pε value can vary as in the following example for the O_2/H_2O couple (O1 in Table 1).

Using the balanced half reaction and the Gibbs free energy of formation of each species at 25°C, the Gibbs free energy of the reaction and the equilibrium constant are calculated.

$$\begin{array}{cccccc} O_{2(aq)} + & 4\ H^+ + & 4e^- \rightarrow & 2H_2O & & \\ 16.32 & 0 & 0 & 2(-237.18) & \Delta G^\circ_{formation}\ (kJ/mol) & \end{array}$$

The standard state ΔG° for the reaction = - 490.68 kJ/2 moles H_2O or 4 moles of electrons. The equilibrium constant (K_4^0) is given in eqn. 2a where {} indicates activity for each chemical species and the activity of H_2O is defined as 1.

$$K_4^0 = \frac{\{H_2O\}^2}{\{O_2\}\ \{H^+\}^4\ \{e^-\}^4} \quad (2a)$$

On expanding, eqn. 2b results.

$$\log K_4^0 = -\log\{O_{2(aq)}\} - \log\{H^+\}^4 - \log\{e^-\}^4 = \frac{\Delta G^0_{reaction}}{2.303\ RT} = 86.00 \quad (2b)$$

$\log K_4^0$ is for 4 mole of electrons or 21.50 for 1 mole of electrons. For a one-electron half-reaction, we have

$$^1/_4O_{2(aq)} + H^+ + e^- \rightarrow {}^1/_2H_2O$$

And equation 2b becomes equation 2c

$$\frac{1}{4}\log K_4^0 = -\frac{1}{4}\log\{O_{2(aq)}\} - \log\{H^+\} - \log\{e^-\} \quad (2c)$$

or

$$\frac{1}{4}\log K_4^0 = -\frac{1}{4}\log\{O_{2(aq)}\} + pH + p\varepsilon \quad and\ \ on\ \ rearranging$$

$$p\varepsilon = \frac{1}{4}\log K_4^0 + \frac{1}{4}\log\{O_{2(aq)}\} - pH$$

From the Nernst Equation, $p\varepsilon^o = 1/4 \log K_4^0 = 21.50$ (the standard state value), which on substitution gives equation O1 (see Table 1) where concentration is used for $O_{2(aq)}$.

TABLE 1 Reduction half-reactions for relevant species of oxygen, nitrogen, sulfur, manganese, iron and iodine normalized to one electron.

OXYGEN REACTIONS		
four electron reaction normalized to one electron		
$¼\ O_{2(aq)} + H^+ + e^- \rightarrow ½H_2O$	$pε = 21.50 - pH + ¼ \log [O_{2(aq)}]$	(O1)
	$pε = pε° - pH = 21.50 - pH$	(O1a)
two electron reactions normalized to one electron		
$½O_{2(aq)} + H^+ + e^- \rightarrow ½H_2O_2$	$pε = pε° - pH = 13.18 - pH$	(O2)
$½H_2O_2 + H^+ + e^- \rightarrow H_2O$	$pε = pε° - pH = 29.82 - pH$	(O3)
$½O_3 + H^+ + e^- \rightarrow ½O_{2(aq)} + ½H_2O$	$pε = pε° - pH = 34.64 - pH$	(O4)
$½{}^1O_{2(aq)} + H^+ + e^- \rightarrow ½H_2O_2$	$pε = pε° - pH = 21.57 - pH$	(O5)
One electron transfer reactions only		
$O_{2(aq)} + e^- \rightarrow O^-_{2(aq)}$	$pε = pε° = -2.72$	(O6)
$O^-_{2(aq)} + 2H^+ + e^- \rightarrow H_2O_2$	$pε = pε° - 2\ pH = 29.08 - 2pH$	(O7)
$H_2O_2 + H^+ + e^- \rightarrow H_2O + OH•$	$pε = pε° - pH = 16.71 - pH$	(O8)
$OH• + e^- \rightarrow OH^-$	$pε = pε° = 28.92 + pOH$	(O9a)
$OH• + H^+ + e^- \rightarrow H_2O$	$pε = pε° = 42.92 - pH$	(O9b)
$^1O_{2(aq)} + e^- \rightarrow O^-_{2(aq)}$	$pε = pε° = 14.04$	(O10)
$O_3 + e^- \rightarrow O^-_3$	$pε = pε° = 17.08$	(O11)
NITROGEN REACTIONS		
two electron reactions (per N) normalized to one electron		
$½NO^-_3 + H^+ + e^- \rightarrow ½NO^-_2 + ½H_2O$	$pε = pε° - pH = 14.28 - pH$	(N1)
$½N_2O + H^+ + e^- \rightarrow ½N_2 + ½H_2O$	$pε = pε° - pH = 29.91 - pH$	(N2)
$½N_2H^+_5 + 1.5H^+ + e^- \rightarrow NH^+_4$	$pε = pε° - 1.5\ pH = 21.56 - 1.5\ pH$	(N3a)
$½N_2H_4 + 2H^+ + e^- \rightarrow NH^+_4$	$pε = pε° - 2\ pH = 25.51 - 2\ pH$	(N3b)
$½NH_3OH^+ + H^+ + e^- \rightarrow NH^+_4 + ½H_2O$	$pε = pε° - pH = 22.83 - pH$	(N4a)
$½NH_2OH + 1.5H^+ + e^- \rightarrow ½NH^+_4 + ½H_2O$	$pε = pε° - 1.5\ pH = 29.77 - 1.5\ pH$	(N4b)
$¼N_2 + 1.25H^+ + e^- \rightarrow ¼N_2H^+_5$	$pε = pε° - 1.25pH = -3.89 - 1.25pH$	(N5)
$½N_2 + H_2O + H^+ + e^- \rightarrow NH_2OH$	$pε = pε° - pH = -22.82 - pH$	(N6)
One electron (per N) transfer reactions only		
$NO^-_3 + 2H^+ + e^- \rightarrow NO_2 + H_2O$	$pε = pε° - 2\ pH = 13.07 - 2\ pH$	(N7)
$NO_2 + e^- \rightarrow NO^-_2$	$pε = pε° = 15.6$	(N8)
$NO_2 + H^+ + e^- \rightarrow HNO_2$	$pε = pε° - pH = 16.51 - pH$	(N8a)
SULFUR REACTIONS		
Two-electron reactions normalized to one electron		
$½S + H^+ + e^- \rightarrow ½H_2S$	$pε = pε° - pH = 2.44 - pH$	(S1)
$½S + ½H^+ + e^- \rightarrow ½HS^-$	$pε = pε° - 0.5\ pH = -1.06 - 0.5\ pH$	(S2)
$½(CH_3)_2SO + H^+ + e^- \rightarrow ½(CH_3)_2S + ½H_2O$	$pε = pε° - 0.5\ pH = 11.56 - pH$	(S3)
One-electron transfer reactions only		
$HS• + e^- \rightarrow HS^-$	$pε = pε° = 18.26$	(S4)
$HS• + H^+ + e^- \rightarrow H_2S$	$pε = pε° - pH = 25.21 - pH$	(S5)
$S + H^+ + e^- \rightarrow HS•$	$pε = pε° - pH = -20.33 - pH$	(S6)

(Continued)

TABLE 1 Continued

MANGANESE REACTIONS		
two electron reactions normalized to one electron		
$½MnO_2 + 2H^+ + e^- \rightarrow ½Mn^{2+} + H_2O$	$pε = pε° - 2\ pH = 20.80 - 2\ pH$	(Mn1)
$½Mn_3O_4 + 4H^+ + e^- \rightarrow 3/2Mn^{2+} + 2H_2O$	$pε = pε° - 4\ pH = 30.82 - 4\ pH$	(Mn2)
One electron transfer reaction only		
$MnOOH + 3\ H^+ + e^- \rightarrow Mn^{2+} + 2\ H_2O$	$pε = pε° - 3\ pH = 25.35 - 3\ pH$	(Mn3)
IRON REACTIONS		
two electron reaction normalized to one electron		
$½Fe_3O_4 + 4H^+ + e^- \rightarrow 3/2Fe^{2+} + 2H_2O$	$pε = pε° - 4\ pH = 18.20 - 4\ pH$	(Fe1)
One electron transfer reactions only		
$FeOOH + 3\ H^+ + e^- \rightarrow Fe^{2+} + 2\ H_2O$	$pε = pε° - 3\ pH = 13.37 - 3\ pH$	(Fe2)
$Fe(OH)_3 + 3\ H^+ + e^- \rightarrow Fe^{2+} + 3\ H_2O$	$pε = pε° - 3\ pH = 18.03 - 3\ pH$	(Fe3)
IODINE REACTIONS		
One electron transfer reaction only		
$½\ I_2 + e^- \rightarrow I^-$	$pε = pε° = 10.50$	(Io1)
two electron reactions normalized to one electron		
$½\ HOI + ½\ H^+ + e^- \rightarrow ½\ I^- + ½\ H_2O$	$pε = pε° - 0.5\ pH = 16.66 - 0.5\ pH$	(Io2)
$HOI + H^+ + e^- \rightarrow ½\ I_2 + H_2O$	$pε = pε° - pH = 22.91 - pH$	(Io3)
$½\ HOIO + H^+ + e^- \rightarrow ½\ HOI + ½\ H_2O$	$pε = pε° - pH = 21.10 - pH$	(Io4a)
$½IO_2^- + 1.5H^+ + e^- \rightarrow ½HOI + ½H_2O$	$pε = pε° - 1.5\ pH = 24.06 - 1.5\ pH$	(Io4b)
$½IO_3^- + 1.5H^+ + e^- \rightarrow ½HOIO + ½H_2O$	$pε = pε° - 1.5\ pH = 17.89 - 1.5\ pH$	(Io5a)
$½IO_3^- + H^+ + e^- \rightarrow ½IO_2^- + ½H_2O$	$pε = pε° - pH = 14.91 - pH$	(Io5b)
six electron reaction normalized to one electron		
$1/6\ IO_3^- + H^+ + e^- \rightarrow 1/6\ I^- + ½H_2O$	$pε = pε° - pH = 18.55 - pH$	(Io6)
	$pε = 18.55 - pH - \frac{1}{6}\ log\frac{[I^-]}{[IO_3^-]}$	

Activities of all reactants other than H^+ are at unity.

$$pε = pε^o + {}^1/_4 log[O_{2(aq)}] - pH = 21.50 + {}^1/_4 log\{O_{2(aq)}\} - pH \quad (O1)$$

At ocean surface conditions of 211 μM O_2 (211 x 10^{-6} M; 100% saturation at 25°C and salinity of 35), this expression becomes

$$pε = 21.50 + {}^1/_4\ log[211 \times 10^{-6}M] - pH = 20.58 - pH$$

and at a pH of 8, pε = 12.58.

At 1μM O_2 (10^{-6} M) which occurs in oxygen minimum zones, this expression becomes

$$pε = 21.50 + {}^1/_4 log[10^{-6}M] - pH \quad = 20.00 - pH$$

and at a pH of 7.5, pε = 12.50.

At unit activity for all reagents including H^+, pε = pε°. At unit activity of all reagents other than the H^+, equation O1a results, which is used for many calculations in this paper.

$$pε = pε^o - pH = 21.50 - pH \quad (O1a)$$

Note that the above equations show a 1.50 log unit change for an O_2 concentration range from 1 μM to unity activity (O1a) so the calculations could vary an order of magnitude or more in either direction when concentration dependence is included. However, comparisons can be more easily made when combining different half-reactions at a given pH. This permits an assessment of which combined half-reactions are thermodynamically favorable and thus more likely to occur in a given environmental setting.

2.2 Coupling half-reactions

As an example of coupling two half reactions to determine whether a reaction is favorable, I use the data in Table 1 for the reduction of IO_3^- (Io5b) by NO_2^- (N1) in equation 3.

$$NO_2^- + IO_3^- \rightarrow NO_3^- + IO_2^- \quad (3)$$

Equation 4 is used to calculate a complete reaction's pε or $\Delta\log K_{reaction}$ value. All values of $\Delta\log K_{reaction} > 0$ indicate a favorable reaction and all values of $\Delta\log K_{reaction} < 0$ indicate an unfavorable reaction.

$$p\varepsilon_{reaction} = p\varepsilon_{red} + p\varepsilon_{oxid} = \Delta\log K_{reaction} \quad (4)$$

At a pH of 7, the $p\varepsilon_{red}$ values for IO_3^- and NO_3^- are 7.91 and 7.28, respectively. As NO_2^- is the reductant, it is oxidized; thus, the sign for $p\varepsilon_{red}$ (7.28) is reversed to become $p\varepsilon_{oxid}$ (-7.28).

$$\Delta\log K_{reaction} = p\varepsilon_{red}(IO_3^-) + p\varepsilon_{oxid}(NO_3^-) = 7.91 + (-7.28) = 0.63$$

For reaction 3, there is no pH dependence as the pH dependence of each half-reaction is similar so cancels.

For this work, Table 1 lists the pε(pH) values for Mn, Fe, oxygen, nitrogen, sulfur and iodine species for the relevant iodine redox reactions considered. Dissolved Fe(II) and Mn(II) are primarily hexaaquo species until the pH is > 7, where hydroxo complexes start to become important. As most reactions occur *via* one and two-electron transfers, the calculations will permit assessment of a thermodynamically unfavorable step along a reaction coordinate of six-electrons as in the reduction of iodate to iodide and the oxidation of iodide to iodate. From surface waters to decomposition zones, seawater pH values range from 8 down to 7; thus, the following discussion will emphasize this pH range.

3 Results and discussion: Iodate reduction

3.1 Iodate and iodide speciation at different seawater oxygen conditions

In the oxic environment, the oxidizing condition of the environment or pε is set by the 4-electron transfer reaction of the $O_{2(aq)}/H_2O$ couple [reaction O1 in Table 1]. At a pH of 8, temperature 25^{0}C and a salinity of 35, 100% $O_{2(aq)}$ saturation is 211 µM, which gives a pε of 12.58 (Figure 1). As the IO_3^-/I^- couple has a pε of 10.56 at pH = 8, IO_3^- is the thermodynamically favored iodine species.

Entering the pε value for a given $[O_{2(aq)}]$ into equation Io6 allows the determination of the iodide to iodate ratio and the actual concentration of each assuming a total iodine concentration of 450-470 nM (Elderfield and Truesdale, 1980). Figure 1 shows the iodate and iodide concentrations are equivalent at a pε of 10.56. The vertical lines indicate the environmental pε for $[O_{2(aq)}]$ of 1, 10, 100 nM, and 1, 50 and 211 µM. As oxygen minimum zones (OMZ) of the Arabian Sea and the equatorial Pacific Ocean have $[O_{2(aq)}]$ concentrations in the 1-100 nM range (Revsbech et al., 2009; Lehner et al., 2015), calculations show that IO_3^- is the thermodynamically preferred iodine species even at 1 nM $O_{2(aq)}$, which gives a pε of 11.25 for the $O_{2(aq)}/H_2O$ couple. However, I^- is the dominant iodine species detected in OMZ waters (Wong and Brewer, 1977; Luther and Campbell, 1991; Rue et al., 1997; Farrenkopf and Luther, 2002; Cutter et al., 2018). At $[O_{2(aq)}]$ concentrations ≤ 1 µM, IO_3^-, NO_3^- and Mn^{2+} concentrations are now similar or higher in concentration and should determine the pε of the water.

As most reactions occur by 1- or 2-electron transfers, Figure 2 shows the redox sequence for two electron transfer redox couples

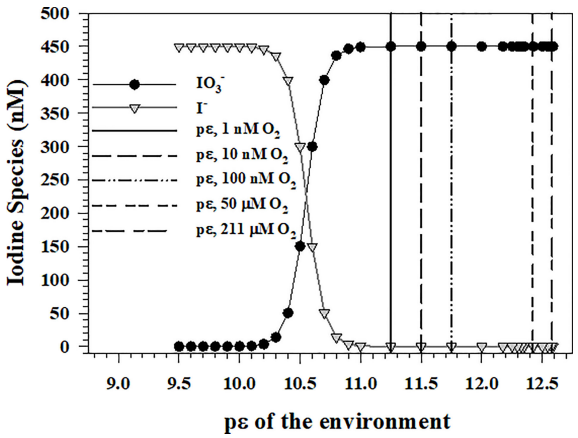

FIGURE 1
IO_3^- and I^- concentrations for a total iodine concentration of 450 nM at different environmental pε values assuming that $O_{2(aq)}$ reduction to H_2O sets the pε value of ocean waters.

NO_3^-/NO_2^-(N1), MnO_2/Mn^{2+} (Mn1) and the one-electron redox couple $Fe(OH)_3/Fe^{2+}$ (Fe3) over a wide range of pH. The redox sequence at pH = 8 is as expected for the N, Mn and Fe systems. As NO_2^- (up to 12 µM) and Mn^{2+} (up to 8 µM) are formed at OMZ oxic-anoxic transition zones (e.g., Arabian Sea, Black Sea, Equatiorial Pacific, see Lewis and Luther, 2000; Trouwborst et al., 2006; Cutter et al., 2018, respectively) and are in higher concentration than $O_{2(aq)}$, the $NO_3^- \rightarrow NO_2^-$(N1) and $MnO_2 \rightarrow Mn^{2+}$ (Mn1) couples can be chosen to set the environmental pε. At pH = 8, the NO_3^- to NO_2^- pε is 6.15 and the MnO_2 to Mn^{2+} pε is 4.80. At pH = 7, the NO_3^- to NO_2^- pε is 7.28 and the MnO_2 to Mn^{2+} pε is 6.80. At these pε values, $O_{2(aq)}$ is below 1 nM, and I^- is now the thermodynamically favored iodine species when comparing these data with the IO_3^-/I^- couple (pε of 10.56 at pH = 8).

Figure 2 also shows that the IO_3^-/IO_2^- couple (Io5b) should be the first step in the reaction sequence of iodate to iodide (eqn. 1a). As the pε of the IO_3^-/IO_2^- couple has a more positive pε value than the N, Mn and Fe couples in Figure 2, IO_3^- reduction is more favorable than these couples even though it is very close to the NO_3^-/NO_2^- couple. Thus, IO_3^- is predicted to reduce before NO_3^-, and biological activity (e.g., nitrate reductase activity) is not necessary to reduce IO_3^- (see section

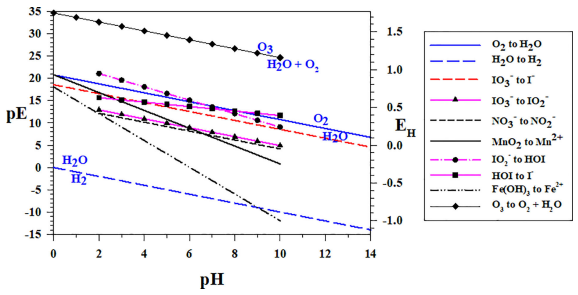

FIGURE 2
Two electron transfer redox couples for O_3 (O4), N (N1), Mn (Mn1) and I (Io2a, Io4b, Io5b), and one electron transfer redox couple for Fe (Fe3). The oxidized species is always above the line and the reduced below the line as in the O_2/H_2O and the H_2O/H_2 couples, which dictate the water stability field.

3.2). Because of the strong pH dependence for the Mn and Fe couples, they cross the IO_3^-/IO_2^- and NO_3^-/NO_2^- couples at lower pH, which have similar slopes. Thus, NO_2^- is predicted to reduce IO_3^- to IO_2^- (eqn. 3). Interestingly, Mn^{2+} and Fe^{2+} should be poorer reductants than NO_2^- for conversion of IO_3^- to IO_2^- at a pH< 6 and pH< 1, respectively, but are more favorable to reduce IO_3^- than NO_2^- above those pH values (see sections 3.2 and 3.3).

Although the IO_3^- to I^- conversion occurs at higher pε, it is a 6-electron transfer (IO6), which is not a facile process. Thus, the intermediates (IO_2^- and HOI) will dictate the reactivity sequence *via* a combination of thermodynamic and kinetic considerations.

As shown in Figure 2, IO_2^- reduction to HOI and HOI reduction to I^- are also more favorable at higher pε values than the IO_3^- to I^- couple. At a pH = 8, the IO_2^- to HOI couple has a pε value of 12.06 corresponding to 2 µM O_2 (see Figure 1). Similarly, the HOI to I^- couple has a pε value of 12.66 corresponding to 250 µM O_2. At a pH of 7, both couples have pε values greater than 13 indicating that, even at O_2 saturation, I^- is the dominant species predicted when these intermediates form. At a pH = 7.5 (that is found in many OMZ waters), both IO_2^- to HOI and HOI to I^- couples have pε values greater than 12.6; also indicating that at O_2 saturation, I^- is the dominant species predicted. Thus, the intermediates IO_2^- and HOI are not predicted to be stable in marine waters; thus, the conversion of IO_3^- to IO_2^- is a key step. Interestingly, Hardisty et al. (2021) found *in situ* IO_3^- reduction in the oxycline where $[O_{2(aq)}]$ was 11 µM, but not at $[O_{2(aq)}]$< 2 µM. Lastly, the O_3 to $O_2 + H_2O$ couple is highly oxidizing indicating that all iodine couples should lead to IO_3^- formation. O_3 reactions will be discussed in more detail below (sections 4.2, 4.7).

In the next sections (3.2 – 3.5), the thermodynamics for the conversion of iodate to iodide *via* the intermediates outlined in equations 1a and 1b by environmental reductants are considered to show what step, if any, in the reduction of iodate to iodide may be unfavorable over a wide range of pH. Iodate reduction is well known in the marine environment (e.g., Wong and Brewer, 1977; Wong et al., 1985; Luther and Campbell, 1991; Rue et al., 1997; Farrenkopf and Luther, 2002; Cutter et al., 2018) and occurs *via* chemical reductants like sulfide (Zhang and Whitfield, 1986) and *via* microbes like *Shewanella putrfaciens* (Farrenkopf et al., 1997) and *Shewanella oneidensis* (Mok et al., 2018) during dissimilatory reduction coupled with decomposition (oxidation) of organic matter as well as phytoplankton mediated processes (e.g., Chance et al., 2007).

3.2 Iodate reduction by NO_2^-

Although NO_2^- has not yet been shown to be a reductant for IO_3^- in aqueous lab studies (eqn. 3), HNO_2 is a reductant for MnO_2 (Luther and Popp, 2002) and Mn(III)-pyrophosphate (Luther et al., 2021). Figure 3A shows the thermodynamic calculations for the stepwise conversion of IO_3^- to I^- by NO_2^- reduction (NO_2^- oxidizes to NO_3^-). All 2-electron transfer reactions, which involve O atom loss for iodine, are favorable over the pH range. For seawater pH (7-8), the least favorable reaction is the IO_3^- to IO_2^- reaction whereas the IO_2^- to HOI and HOI to I^- reactions are more favorable. Thus, the IO_3^- to IO_2^- conversion appears to be the controlling step in the reaction sequence. The 1-electron transfer reaction of HOI to I_2 is the most favorable, but the second 1-electron transfer reaction of I_2 to I^- is only favorable at pH > 4. Thus, reduction of IO_3^- to I^- by NO_2^- is predicted *via* 1-electron or 2-electron transfer reactions at seawater pH values. The data plotted in Figure 2 indicate that once IO_2^- forms there is no thermodynamic barrier to I^- formation.

The IO_3^- reaction with NO_2^- has been reported to produce I_2 in ice by Kim et al. (2019), but not in solution. The pH in the ice was 3 where HNO_2 and H_2ONO^+ exist and are the likely reductants. Thus, polar areas may be locales for IO_3^- reduction. At seawater pH, the reaction seems to be hindered by kinetics in the transition state as each reactant (IO_3^- and NO_2^-) is an anion, which will repel each other.

3.3 Biological iodate reduction

The marine literature has many reports on the uptake of IO_3^- (with or without NO_3^-) by phytoplankton with the iodine released as I^- (e.g., Elderfield and Truesdale, 1980; Wong, 2001; Wong et al., 2002; Chance et al., 2007; Bluhm et al., 2010). As a result of this iodate uptake, NO_3^- reductase was presumed by some researchers to be a key process for IO_3^- reduction to I^-. Also, Bluhm et al. (2010) and Carrano et al. (2020) showed that algal senescence enhanced I^- release, and Hepach et al. (2020) showed that there is a considerable lag between IO_3^- uptake and I^- release due to senescence.

NO_3^- reductase appears to reduce IO_3^- in some phytoplankton (Hung et al., 2005). However, de la Cuesta and Manley (2009) showed that I^- can be up taken by phytoplankton, and that different phytoplankton uptake I^- whereas other phytoplankton uptake IO_3^-. Thus, there is no need for nitrate reductase for IO_3^- reduction as I^- can be up taken by some phytoplankton rather than form from IO_3^- reduction. Moreover, Waite and Truesdale (2003) showed that nitrate reductase was not important for IO_3^- reduction by *Isochrysis galbana*. The latter study is consistent with the thermodynamics of the reduction IO_3^- to IO_2^- being more favorable than the reduction NO_3^- to NO_2^-.

Furthermore, under anaerobic conditions, dissimilatory IO_3^- reduction occurs without nitrate reductase for the denitrifying bacterium, *Pseudomonas stutzeri*, (Amachi et al., 2007; Amachi, 2008). Reyes-Umana et al. (2022) and Yamazaki et al. (2020) showed that iodate reductase is in the periplasmic space of *Pseudomonas sp* SCT. Also, Mok et al. (2018) showed that dissimilatory IO_3^- reduction by *Shewanella oneidensis* does not involve nitrate reductase. Recently, Shin et al. (2022) showed that *Shewanella oneidensis* requires extracellular dimethylsulfoxide (DMSO) reductase involving a molybdenum enzyme center for IO_3^- reduction. Guo et al. (2022) studied bacterial genomes in a variety of environments and documented that *Shewanella oneidensis* are ubiquitous in all fresh and marine waters; they concluded that IO_3^- reduction is a major biogeochemical process. Thus, nitrate reductase (also an O atom transfer reaction) is not a requirement for bacterial IO_3^- reduction to I^-.

The interconversion of dimethylsulfoxide with dimethylsulfide during dissimilatory IO_3^- reduction is another 2-electron O-atom transfer reaction. Moreover, the reactions of DMS to reduce HOI, IO_2^- and IO_3^- are thermodynamically favorable (Figure 3B, DMSO reduction is in S3, Table 1 and occurs at a lower pε than NO_3^- and IO_3^- reduction). The reaction of DMS with HOI has been suggested by

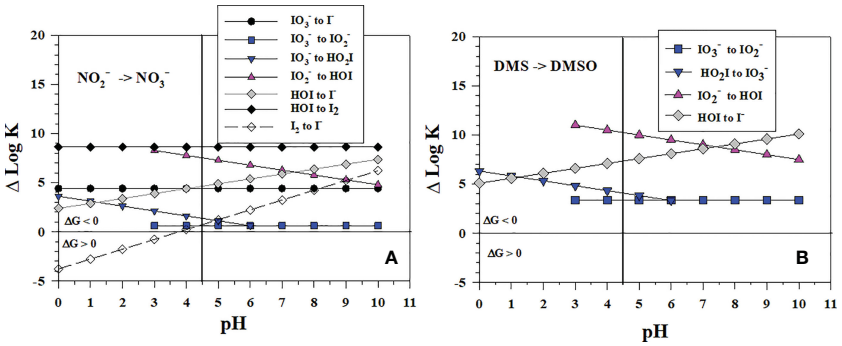

FIGURE 3
Thermodynamics for **(A)** the 1-electron and 2-electron reductions of IO_3^- (Io5a, Io5b, Io6), IO_2^- (Io4b), HOI (Io2, Io3), and I_2 (Io1) by NO_2^- (N1) and **(B)** 2-electron reductions of IO_3^- (Io5b), IO_2^- (Io4a, Io4b), HOI (Io2) by DMS (S3). The vertical line represents the pK_a value of 4.49 for HO_2I. Data above the horizontal line at ΔlogK ($\Delta logK_{reaction}$) = 0 indicate a favorable reaction and data below the horizontal line indicate an unfavorable reaction.

Müller et al. (2021) to be a sink for DMS based on the rapid reaction of DMS with HOBr.

3.4 Iodate reduction by Mn^{2+} and Fe^{2+}

Figure 4 shows the thermodynamics for the stepwise conversion of IO_3^- to I^- by reduction with Mn^{2+} and Fe^{2+}. Concentrations of Mn^{2+} and Fe^{2+} range from several nM to µM in OMZs (e.g., Trouwborst et al., 2006; Moffett and German, 2020) and in suboxic porewaters (e.g., Oldham et al., 2019; Owings et al., 2021) to mM in waters emanating from hydrothermal vents (e.g., Estes et al., 2022); in these cases, Mn^{2+} and Fe^{2+} are normally higher in concentration than the total iodine concentration. For the 2-electron transfer reactions with Mn^{2+}, only the IO_2^- to HOI reaction is favorable over the entire pH range. The IO_3^- to IO_2^- reaction is favorable only at pH > 6 whereas the other reactions are favorable at pH > 3. Thus, the IO_3^- to IO_2^- conversion is the controlling step in the reaction sequence when Mn^{2+} is the reductant. Using high resolution porewater profiles of I^- and Mn^{2+} obtained by voltammetric microelectrodes, Anschutz et al. (2000) showed that a I^- maximum occurred at the depth where upward diffusing Mn(II) was being removed and proposed that I^- formed by the reaction of IO_3^- with Mn^{2+} under suboxic conditions. The reaction has not been investigated in laboratory studies.

For the reaction sequence with Fe^{2+}, all iodine species reductions are favorable over the entire pH range except for the I_2 to I^- reaction, which is favorable at pH > 2.5. Thus, there is no thermodynamic inhibition to IO_3^- reduction to I^- by Fe^{2+}, and this abiotic reaction at a pH of 7 was reported to be 92% complete after 2 hours using initial concentrations of 2 mM Fe^{2+} and 0.1 mM IO_3^- (Councell et al., 1997). Because the $Fe(OH)_3$ to Fe^{2+} couple is a 1-electron transfer, two Fe^{2+} are required in each step of the sequence. Again, the IO_3^- to IO_2^- conversion is the least favorable and likely controlling step in this reaction sequence.

Comparing Figures 3, 4 indicates that the Mn^{2+} and NO_2^- reactions with iodine species have a similar range of $\Delta logK_{reaction}$ values whereas the Fe^{2+} reactions with iodine species are more favorable (higher $\Delta logK_{reaction}$ values).

3.5 Iodate reduction by sulfide

In sulfidic waters and porewaters, IO_3^- does not exist as sulfide reacts readily with it (Zhang and Whitfield, 1986), and S(0) forms as the initial sulfur product. Figure 5 shows the thermodynamics for the stepwise conversion of IO_3^- to IO_2^- and to HOI by sulfide where S(0) forms as an intermediate leading to S_8. As the Gibbs free energy of formation for HSOH is unknown, HSOH could not be evaluated as an

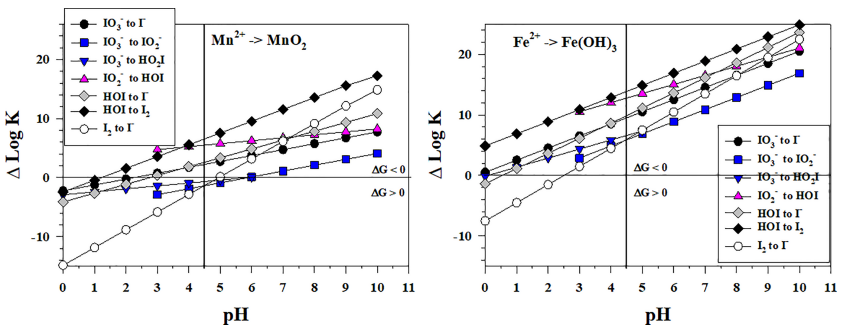

FIGURE 4
Thermodynamics for the reduction of IO_3^- (Io5a, Io5b, Io6), IO_2^- (Io4b), HOI (Io2, Io3), and I_2 (Io1) by Mn^{2+} (Mn1) and Fe^{2+} (Fe3). The vertical line represents the pK_a value of 4.49 for HO_2I. Data above the horizontal line at ΔlogK ($\Delta logK_{reaction}$) = 0 indicate a favorable reaction and data below the horizontal line indicate an unfavorable reaction.

intermediate, which on continued oxidation would form SO_4^{2-}. The reaction of sulfide with I_2 and HOI is well known as the iodometric titration, so calculations were not performed. The only unfavorable iodine reduction reactions are the 1-electron reductions that lead to the formation of the HS radical (HS• or HS rad). The conversion of IO_2^- to HOI is more favorable as it has the larger $\Delta logK_{reaction}$ values. Again, the IO_3^- to IO_2^- conversion is the least favorable and likely controlling step in this reaction sequence.

3.6 Iodate reduction by NH_4^+

Figure 6 shows the thermodynamics for the stepwise conversion of IO_3^- to IO_2^- by NH_4^+ where hydrazine (N_2H_4) and hydroxylamine (NH_2OH) as well as their protonated forms could form as the first N intermediates. The thermodynamic calculations for these 2 electron transfers indicate that these reactions are not favorable. However, the reaction of the intermediates, if they could form by other processes, with IO_3^- to form N_2 is very favorable. Thus, the IO_3^- to IO_2^- conversion is the controlling step in the reaction sequence with NH_4^+.

4 Results and discussion: Iodide oxidation

4.1 Iodide oxidation by NO_3^-, MnO_2 and $Fe(OH)_3$

Figures 3–6 showed the reduction of IO_3^- with reductants. All values of $\Delta logK_{reaction} > 0$ indicate a favorable reaction and all values of $\Delta logK_{reaction} < 0$ indicate an unfavorable reaction. These figures can be used to discuss the reverse reaction of I^- oxidation with oxidants. For reverse reactions, when a $\Delta logK_{reaction} < 0$, then I^- oxidation is favorable, but when $\Delta logK_{reaction} > 0$, I^- oxidation is unfavorable.

In Figure 3, NO_3^- is not an oxidant for I^- (reverse of the NO_2^- and I_2 reaction) except for the formation of I_2 at a pH< 4.

In Figure 4, MnO_2 oxidizes I^- to HOI (reverse of the Mn^{2+} and HOI reaction) at a pH< 3 and I^- to I_2 (reverse of the Mn^{2+} and I_2 reaction) at a pH< 5. A couple of laboratory studies showed I^- oxidation with synthetic birnessite (δ-MnO_2). First, Fox et al. (2009) showed that I_2 was produced over the pH range 4.50 – 6.25, and that IO_3^- formed in smaller amounts. The kinetics of the reaction were slower at higher pH by 1.5 log units (> 30-fold) and were slower when smaller amounts of MnO_2 were added (Table 2). Allard et al. (2009) investigated the same reactants to a pH of 7.5 and found I_2 and IO_3^- as products; above pH = 7 the reaction is very slow. Iodate was found mainly in lower pH waters. Both I_2 and IO_3^- adsorb to the birnessite surface. Similar results have been found over the pH range 4-6 for Mn(III) solids (Szlamkowicz et al., 2022). These MnO_x reactions with I^- are much slower that the reactions with reactive oxygen species (Table 2). Nevertheless, these are important as Kennedy and Elderfield (1987a, 1987b) showed that the conversion of iodide to iodate occurred in marine sediments.

Figure 4 also shows that I^- oxidation by $Fe(OH)_3$ to I_2 (reverse of the Fe^{2+} and I_2 reaction) should occur only at a pH< 2.5. The I^- to HOI conversion (reverse of the Fe^{2+} and HOI reaction) is favorable at pH ≤ 0.5.

4.2 Iodide oxidation by oxygen species

Figure 7 shows the thermodynamics of I^- oxidation to I_2 by oxygen species. Figure 7A shows that the one-electron process for I^- oxidation with $^3O_2$ is thermodynamically unfavorable over all pH whereas Figure 7B shows that the two-electron process is favorable at a pH< 3. Figure 7A shows that the successive 1-electron oxidations of I^- where superoxide (O_2^-) is reduced to hydrogen peroxide (H_2O_2), which is reduced to hydroxyl radical (•OH). Only •OH is thermodynamically favorable over the pH range considered. O_2^- and H_2O_2 show favorable reactions at pH< 9 and pH< 6, respectively.

By contrast, Figure 7B shows that the reactions of I^- with the 2-electron oxidants H_2O_2, $^1O_2$ and O_3 are all thermodynamically favorable. The likely reaction pathway is the loss of 2-electrons to produce I^+, which then reacts with I^- to form I_2. Note that H_2O_2 reacts to form H_2O not •OH in Figure 7B. The 2-electron reaction with O_3 (Figure 7B) is more favorable than the 1-electron reaction (Figure 7A).

Wong and Zhang (2008) showed that H_2O_2 oxidizes I^- in artificial seawater from pH 7-9, which is consistent with Figure 7B. However, I^- oxidation does not lead to iodate. In fact, I^- reforms. They proposed that I_2 formed and was reduced back to I^-, but they did not provide a mechanism. The reverse reaction of I_2 with •OH ($\Delta logK_{reaction} < 0$ in

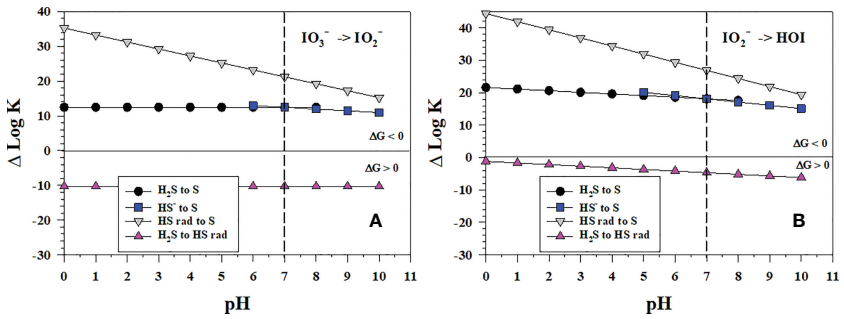

FIGURE 5
Thermodynamics for the 2-electron transfer reductions of **(A)** IO_3^- (Io5b) and **(B)** IO_2^- (Io4b) by sulfide species (S1, S2, S4, S5). The vertical line represents the pK_{a1} value for H_2S. Data above the horizontal line at ΔlogK ($\Delta logK_{reaction}$) = 0 indicate a favorable reaction and data below the horizontal line indicate an unfavorable reaction.

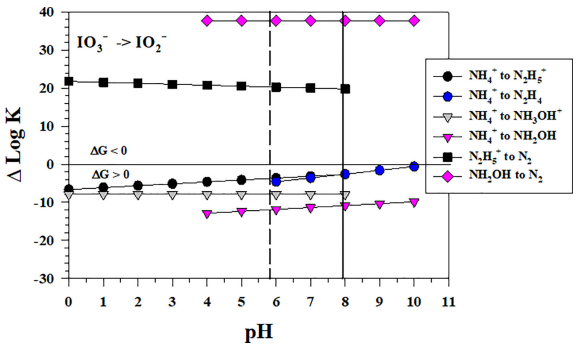

FIGURE 6
Thermodynamics for the reduction of IO_3^- to IO_2^- (IO5b) by NH_4^+ to hydrazine species (N3a, N3b), hydroxylamine species (N4a, N4b) and by $N_2H_5^+$ (N5) and NH_2OH (N6). The vertical lines represent the pK_a values for NH_3OH^+ (5.82) and $N_2H_5^+$ (7.93), respectively. Data above the horizontal line at ΔlogK ($\Delta logK_{reaction}$) = 0 indicate a favorable reaction and data below the horizontal line indicate an unfavorable reaction.

the plot) is favorable to reform H_2O_2 and I^- at pH > 6 whereas the reverse reaction of H_2O_2 with I_2 to reform O_2^- and I^- is favorable at a pH > 9 ($\Delta logK_{reaction} < 0$ in the plot). These thermodynamic data indicate that H_2O_2 can form I_2 in a 2-electron transfer (Figure 7B) and then reduce I_2 to I^- in a 1-electron transfer (Figure 7A).

At seawater pH, superoxide, O_2^-, can oxidize I^- to I_2 and the reaction occurs with a rate constant of 10^8 $M^{-1}s^{-1}$ (Bielski et al., 1985; Table 2). Because I_2 is a good electron acceptor, the subsequent reaction of O_2^- with I_2 leads to I_2^- (Schwarz and Bielski, 1986). As to be discussed in section 4.3, I_2 reacts with organic matter to form organo-iodine compounds. Extracellular O_2^- is generated by *Roseobacter* sp. AzwK-3b (Li et al., 2014) and results in the oxidation of Mn^{2+} to Mn (III,IV) oxides. However, Li et al. (2014) found that O_2^- also oxidized I^-. Considering that extracellular O_2^- formation is a widespread phenomenon among marine and terrestrial bacteria, this could represent an important first step in the pathway for iodide oxidation in some environments. The Mn oxides formed by *Roseobacter* sp. AzwK-3b are not the oxidant as MnO_2 kinetics is slower (Table 2).

To obtain IO_3^-, further oxidation of I_2 to HOI must occur, and •OH is one candidate with a rate constant of 1.2 x 10^{10} (Buxton et al., 1988; Table 2). Also, O_3 has a rate constant of 1.2 x 10^9 (Liu et al., 2001).

I_2 is a prominent intermediate in I^- oxidation yet HOI is needed to form IO_3^-. HOI can form directly from I^- and I_2 oxidation or from hydrolysis of I_2 (reverse of eqn. 5), which is fast at basic pH (Wong, 1991). Figure 8A shows that of the successive 1-electron oxidants (starting from O_2) for I_2 oxidation, only •OH is thermodynamically favorable over all pH to form HOI whereas O_3 is favorable at pH > 6, and O_2^- is favorable at pH< 6. H_2O_2 as a 1-electron oxidant cannot oxidize I_2 to form HOI, but H_2O_2 can reduce HOI to I_2 (reverse of the O_2^- and I_2 reaction). Figure 8B indicates that, as 2-electron oxidants, H_2O_2 and O_3 oxidation can lead to HOI formation. Comparing Δlog K values in Figures 7, 8 indicates that oxidation of I_2 to HOI is less favorable than the oxidation of I^- to I_2.

These data also indicate why the comproportionation reaction of HOI with I^- to form I_2 can occur (eqn. 5, Carpenter et al., 2013).

$$H^+ + HOI + I^- \leftrightarrow I_2 + H_2O \quad (5)$$

Although disproportionation of HOI to IO_3^- and I^- (eqn. 6) is fast in strongly basic solution, it is not detectable at seawater pH (Wong, 1991).

$$3HOI + 3OH^- \leftrightarrow IO_3^- + 2I^- + 3H_2O \quad (6)$$

Figure 9 shows the successive 2-electron oxidation reactions of I^-, HOI and IO_2^- with $^3O_2$, $^1O_2$, H_2O_2 and O_3. $^3O_2$ cannot affect the oxidation at any pH. Figure 9 shows that O_3 oxidation reactions with I^-, HOI and IO_2^- are favorable; thus, O_3 can affect the complete oxidation of I^- to IO_3^-. Also, the H_2O_2 oxidation reactions of I^-, HOI and IO_2^- are favorable and can lead to IO_3^- formation; however, the kinetics of H_2O_2 oxidation can be slow. Haloperoxidase enzymes from organisms enhance the kinetics (Butler and Sandy, 2009) as does the reaction of H_2O_2 with carboxylic acids secreted by microbes to form peroxy carboxylic acids, which in turn oxidize I^- to I_2 (Li et al., 2012). The reactive oxygen species $^1O_2$ can oxidize I^- at pH< 10, oxidize HOI at pH > 5, and IO_2^- over all pH. Thus, $^1O_2$ can be an oxidant of I^- to IO_3^- at seawater pH. These data indicate that HOI oxidation leads to IO_3^- formation.

Interestingly, ΔlogK values in Figure 9A show that the thermodynamics of I^- oxidation by the 2-electron oxidants O_3 and H_2O_2 to form HOI is slightly less favorable than I_2 formation

TABLE 2 Kinetic rate constants for the reaction of oxidants with Iodide and I_2.

I^- with oxidant	k_{12} (M^{-1} s^{-1})	reference
O_3	1.2 x 10^9	Liu et al. (2001)
$^1O_2$	8.7 x 10^5 - 8.7 x 10^6	Wilkinson et al. (1995), p. 896, pH ~ 7
•OH	1.2 x 10^{10}	Buxton et al. (1988) p. 527, 684
O_2^-/HO_2	1 x 10^8	Bielski et al. (1985), p. 1063
H_2O_2	0.69	Mohammed and Liebhafsky (1934)
MnO_2	3 x 10^3 (M^{-2} s^{-1})	Fox et al. (2009) includes pH dependence
I_2 with oxidant		
HO_2	1.8 x 10^7	Schwarz and Bielski (1986)

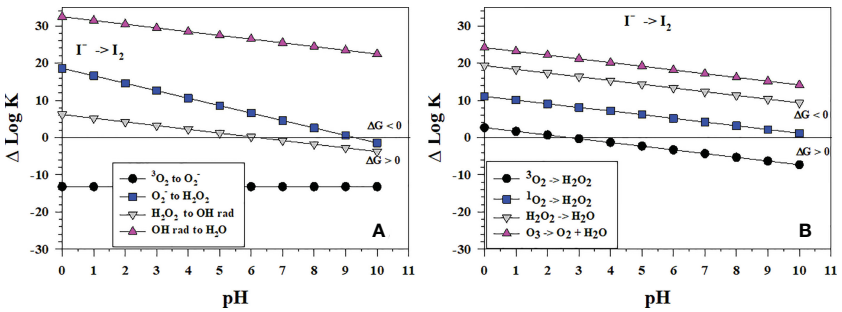

FIGURE 7
Thermodynamics for I_2 formation *via* the oxidation of I^- (Io1) with **(A)** the successive 1-electron oxidants $^3O_2$ (O6), O_2^- (O7), H_2O_2 (O8) and •OH (O9b); **(B)** the 2-electron oxidants $^3O_2$ (O2), $^1O_2$ (O5), H_2O_2 (O3), and O_3 (O4). Data above the horizontal line at ΔlogK ($\Delta logK_{reaction}$) = 0 indicate a favorable reaction and data below the horizontal line indicate an unfavorable reaction.

(Figure 7B). Conversely, thermodynamics of I^- oxidation by H_2O_2 as a 2-electron oxidant to form HOI (Figure 9A) is more favorable than I_2 formation (Figure 7A).

As shown in Figure 10, a potentially potent oxidant for I^- is N_2O, which is an O atom transfer oxidant like O_3. However, the N_2O concentration in seawater is minor, but the largest reported values are 90 and 250 nmol kg^{-1} for the OMZs of the Arabian Sea (Freing et al., 2012) and the Eastern Tropical North Pacific (Damgaard et al., 2020), respectively. These values are smaller than the total iodine concentration in seawater. The N_2O concentration in the atmosphere is 335 ppbv (August 2022, https://www.n2olevels.org), which is equivalent to 0.0331 Pa or 7.8 nM dissolved in surface seawater (salinity of 35) at 20 ^{0}C using the solubility data from Weiss and Price (1980).

4.3 ROS in seawater

Reactive oxygen species exist in marine waters, but at low concentrations. O_3 penetrates a few micrometers through the water-air interface at surface iodide concentrations (Carpenter et al., 2013). Powers and Miller (2014) showed that solar-induced processes with organic matter in freshwater and seawater are a major source of ROS (as O_2^-, H_2O_2, and •OH) with the inventory and production rates for H_2O_2 in surface seawater being highest of the ROS. Also, Sutherland et al. (2020) report that dark, extracellular O_2^- production is prolific among marine heterotrophic bacteria, cyanobacteria, and eukaryotes. In surface ocean waters, the concentration of H_2O_2 ranges from 20 - 80 nM (Yuan and Shiller, 2001), biological O_2^- production gives a total concentration of ~ 0.07 to 0.30 nM (Sutherland et al., 2020), •OH concentration is ~10^{-18} M (Mopper and Zhou, 1990), and $^1O_2$ concentration ranges from 10^{-13} to 10^{-14} M (Sunday et al., 2020). However, these ROS concentrations are typically smaller than I^- concentrations, which range from 10 to 200 nM (Chance et al., 2019). Thus, I^- oxidation in seawater samples should be difficult to observe experimentally. Hardisty et al. (2020) tracked the addition of stable isotopes of iodide in sample incubations and report the rate of I^- oxidation to be 118–189 nM yr^{-1}, which is similar to rates reported by mass balance approaches (Campos et al., 1996a; Truesdale et al., 2001; Žic and Branica, 2006; Žic et al., 2008). Hardisty et al. (2020) report that the product is likely HOI that results in the formation of organic-iodine compounds (see section 4.6) which on decomposition can release I^-.

As the surface concentrations of ROS are smaller than the I^- concentration, the question is how does I^- get oxidized to IO_3^- in seawater? Microbial processes and the oxidation of I species in the atmosphere by ROS are likely candidates. These are now discussed.

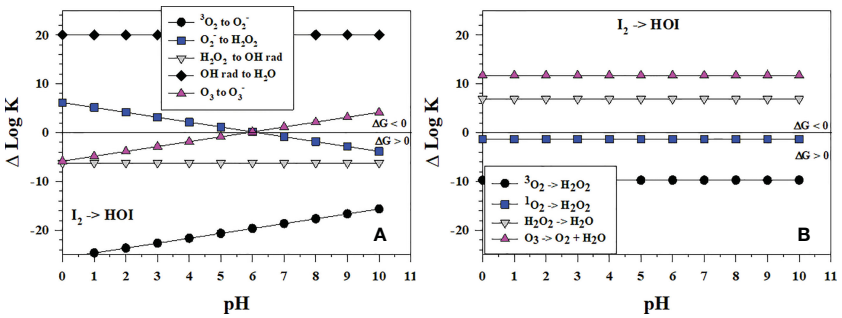

FIGURE 8
Thermodynamics for the formation of HOI *via* the oxidation of I_2 (Io3) with **(A)** the successive 1-electron oxidants $^3O_2$ (O6), O_2^- (O7), H_2O_2 (O8), •OH (O9b) and O_3 (O11); **(B)** the 2-electron oxidants $^3O_2$ (O2), $^1O_2$ (O5), H_2O_2 (O3), and O_3 (O4). Data above the horizontal line at ΔlogK ($\Delta logK_{reaction}$) = 0 indicate a favorable reaction and data below the horizontal line indicate an unfavorable reaction.

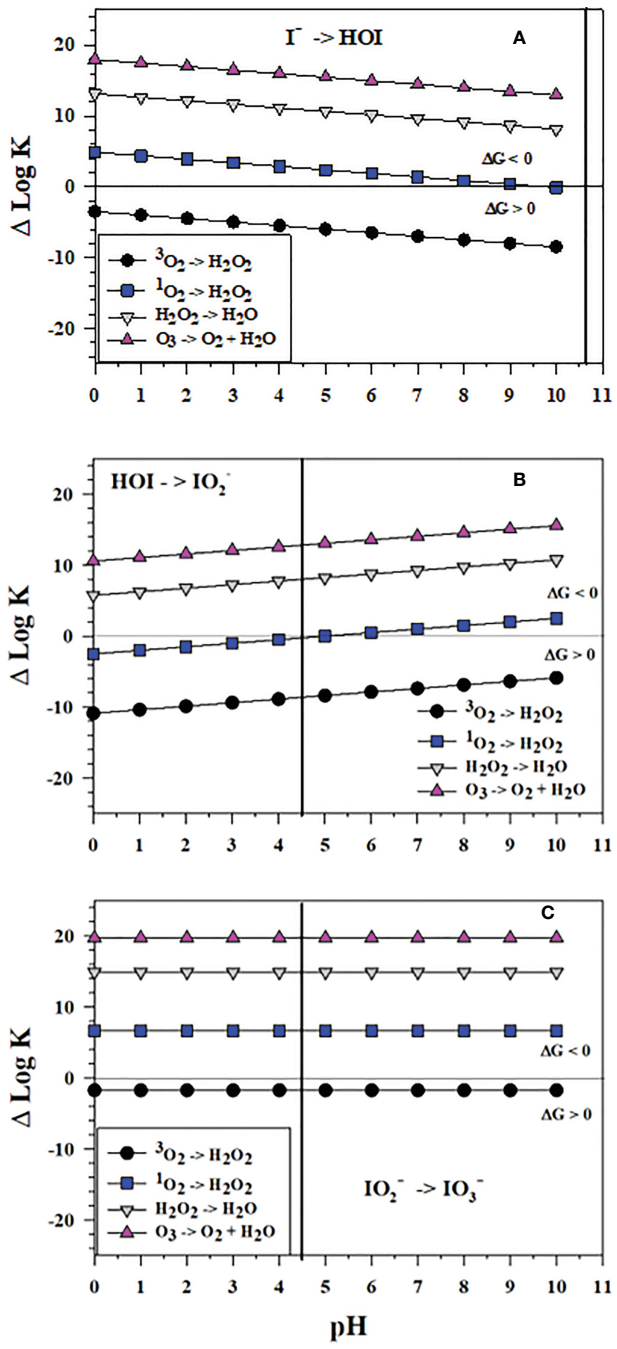

FIGURE 9
Thermodynamics for the reaction of $^3O_2$ (O2), $^1O_2$ (O5), H_2O_2 (O3), and O_3 (O4) as 2-electron oxidants with **(A)** I^- to form HOI (Io2), **(B)** HOI to form IO_2^- (Io4b) and **(C)** IO_2^- to form IO_3^- (Io5b). The vertical lines represent the pK_a value of 4.49 for HO_2I dissociation to IO_2^-. Data above the horizontal line at ΔlogK ($\Delta logK_{reaction}$) = 0 indicate a favorable reaction and data below the horizontal line indicate an unfavorable reaction.

4.4 Iodide oxidation in brown kelp

Brown kelp are the strongest accumulators of iodine as I^- among living organisms (up to 100 mM, Küpper et al., 2008). The element iodine was discovered by the formation of I_2 during exposure of brown kelp to concentrated sulfuric acid, which oxidized I^- to I_2. Kelp

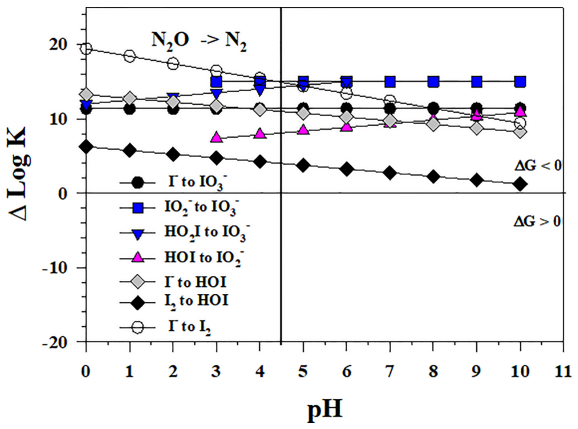

FIGURE 10
Thermodynamics for the 1- and 2- electron reductions of IO_3^- (Io5a, Io5b, Io6), IO_2^- (Io4b), HOI (Io2, Io3), and I_2 (Io1) by N_2O (N2). Data above the horizontal line at ΔlogK ($\Delta logK_{reaction}$) = 0 indicate a favorable reaction and data below the horizontal line indicate an unfavorable reaction.

releases I^- on the thallus surface and in the apoplast when undergoing oxidative stress during the partial emersion of the brown kelp forest at low tide; e.g., by exposure to high irradiance, desiccation, and atmospheric O_3. Kelp contain vanadium haloperoxidases (Colin et al., 2003; Küpper et al., 2008) that enhance I^- oxidation by H_2O_2. Whereas the nonenzymatic reaction of I^- with H_2O_2 is slow, the reactions with O_3, O_2^-, $^1O_2$, and •OH are very fast (> 10^8 $M^{-1}s^{-1}$, Table 2); they are also faster than MnO_2 oxidation of I^-. Küpper et al. (2008) consider I^- as the simplest antioxidant known.

4.5 Iodide oxidation by microbes

Hughes et al. (2021) report that IO_3^- production occurs in cultures of the ammonia-oxidizing bacteria *Nitrosomonas* sp. and *Nitrosococcus oceani* supplied with I^-, but not in cultures of three different nitrite oxidizing bacteria. Information on the enzymes mediating the oxidation were not studied. Nevertheless, NH_4^+ oxidation *via* nitrification occurs *via* NH_2OH formation which is a 2-electron reaction. Further reaction of NH_2OH *via* metalloenzymes (e.g., Mo and W oxidases that transfer O atoms) leads to NO_2^- (a 4-electron transfer) and NO_3^-. I^- likely goes through the intermediates IO_2^- and HOI to form IO_3^-, but these intermediates are reactive and not detectable by present analytical methods unlike NO_2^-.

Consistent with the Hughes et al. (2021) report, Kennedy and Elderfield (1987a, 1987b) showed that the conversion of iodide to iodate occurred in marine sediments. Microbial intervention is likely, but reaction of I^- with oxidized Mn is possible depending on the pH.

Amachi and Iino (2022) reviewed the genus *Iodidimonas*, which was originally found in brines, but was also cultured from seawater enriched with I^-. I_2 is the first oxidation product. *Iodidimonas* contains the iodide oxidizing enzyme (IOX), which is an extracellular protein that contains multicopper oxidases. *Iodidimonas* requires O_2, not H_2O_2, as the electron acceptor. Other oxidants are required to oxidize I_2 to IO_3^- with O_3 and •OH being the most effective.

4.6 HOI and I_2 formation leads to organic iodine

Competing with the inorganic interconversion between iodide and iodate is the formation of organic iodine compounds. Formation of C-I bonds can occur during the reduction of IO_3^- and oxidation of I^-. Complete reduction of IO_3^- to I^- does not need to occur intercellularly and can lead to HOI and I_2 formation as in Figure 4. The first step in I^- oxidation also leads to I_2 and HOI. I_2 is neutral and adds to organic compounds such as olefins, which are not very reactive in seawater, whereas I^+ in HOI reacts with α-keto compounds and peptides through keto-enol isomerization (Truesdale and Luther, 1995). Both I_2 and HOI lead to volatile and nonvolatile organic-iodine (R-I) compounds with C-I or N-I bonds, and Harvey (1980) showed that N-iodo amides were the main organic iodine components in marine sediments. On decay of organic compounds, the C(N)-I bond breaks leading to I^- release, which mimics the senescence pathway outlined by Bluhm et al. (2010) and Hepach et al. (2020). Recently, Ooki et al. (2022) showed that CH_3I and CH_3CH_2I formed in sediments from polar and subpolar seas and was related to increased phytodetritus at the seafloor after the spring bloom.

Allard and Gallard (2013) showed that the oxidation of I^- by birnessite in the presence of organic matter also led to CH_3I over the pH range 4-5.

As total iodine in surface ocean waters is lower by a few percent compared to deep waters (Wong, 1991), the decomposition of organic-iodine leads to some I^- release, which may be oxidized to IO_3^- by ammonia-oxidizing bacteria (Hughes et al., 2021). This is similar to release and oxidation of NH_4^+ to NO_3^- from particulate organic matter in deep waters that results in an increase of NO_3^- concentration with depth (recycled element profile). Deep waters contain mainly IO_3^-, so not much I^- is released to the deep-water column by *in situ* water column processes, and most organic-iodine gets to the sediments where it is released as I^- (Kennedy and Elderfield, 1987a, Kennedy and Elderfields 1987b; Luther et al., 1995). Kennedy and Elderfield (1987a, 1987b) and Shimmield and Pedersen (1990) report that the molar I/C ratio in planktonic organisms is 10^{-4} whereas it is typically $>10^{-3}$ in sediments. Decomposition of sedimentary organic-I releases I^- to porewaters and the overlying water column where it can be transported hundreds of kilometers offshore along isopycnal surfaces in OMZs (Farrenkopf and Luther, 2002; Cutter et al., 2018).

4.7 Surface seawater and atmospheric formation of IO_3^-, and iodine speciation in the atmosphere

There is significant literature showing that coastal and oceanic regions are sources of iodine emissions to the atmosphere, and I note some important aspects of this air-sea connection. I^- reacts with O_3 to form IO^-, which at seawater pH forms HOI. Carpenter et al. (2013) showed that this reaction occurs in the first few micrometers below the air-water interface and that HOI is ten-fold greater than I_2 above the sea surface. HOI contributes 75% of the observed iodine oxide aerosol levels over the tropical Atlantic Ocean, and these iodine emissions to the atmosphere have increased 3-fold over the last century due to the increase in anthropogenic O_3 (Carpenter et al., 2021). O_3 reacts stepwise with this gaseous HOI (IO^-) and gaseous IO_2^- to form IO_3^-, which can attach to aerosols.

Formation and release of gaseous I_2 from seawater to air permits photochemical breaking of the I-I bond to form gaseous I atoms, •I, which are reactive radicals. Similarly, release of volatile organic-iodine compounds leads to the homolytic cleavage of the C-I bond to form I•. O_3 reacts readily with I• to form gaseous IO• in the marine boundary layer (Whalley et al., 2010). Further stepwise oxidation of gaseous IO•/HOI leads to IO_3^-. In laboratory experiments using mass spectrometry detection, Teiwes et al. (2019) showed that hydrated iodide, $I(H_2O)^-$, reacts with gaseous O_3 to form IO_2^- directly without formation of gaseous HOI or IO^-; thus, HIO_3/IO_3^- can form in a two-step reaction sequence in the atmosphere.

Using mass spectrometry to evaluate atmospheric I_xO_y cluster and (nano)particle formation above seabed macroalgae, Sipilä et al. (2016) showed the stepwise formation of HIO_3 *via* HOI and IO•, which leads to $(I_2O_5)_x$ clusters (x=2-5) containing HIO_3 that result in iodine rich aerosol particles. These data on the formation of I_2O_5 aerosols agree with the exothermic $\Delta H_{reaction}$ values of iodine oxide species reacting with O_3 and each other calculated using quantum mechanics (Kaltsoyannis and Plane, 2008). Sipilä et al. (2016) also showed that cluster formation increased as a burst at low tide indicating significant I_2 release from the macroalgae (and subsequent oxidation) as found by Küpper et al. (2008). Hydration of I_2O_5 leads to two IO_3^-. In mass spectrometry laboratory studies, Martín et al. (2022) showed that new iodine containing (nano) particles and IO_3^- also form in the presence of NO_3^- and provide $\Delta H_{reaction}$ data for the gas phase reactions involved. Experiments using the CERN CLOUD (Cosmics Leaving Outdoor Droplets) chamber documented the formation of HIO_3 *via* iodooxy hypoiodite, IOIO, as an intermediate (Finkenzeller et al., 2022) and the fast growth of HIO_3 as (nano)particles (He et al., 2021).

In recent atmospheric campaigns, Koenig et al. (2020) showed that IO_3^- is the main iodine reservoir as it forms on aerosols in the stratosphere with iodine being responsible for 32% of the halogen induced O_3 loss. Cuevas et al. (2022) also showed that iodine can dominate (~73%) the halogen-mediated lower stratospheric ozone loss during summer and early fall, when the heterogeneous reactivation of inorganic chlorine and bromine reservoirs is reduced.

The information in the preceding paragraphs along with the thermodynamic data from Martín et al. (2022), Figure 2 (the half reaction for O_3 to O_2 and H_2O) and Figure 9 predict that IO_3^- should be the dominant species in the atmosphere. Although reduction of IO_3^- is not predicted in an oxidizing atmosphere, analyses of rainwater (Campos et al., 1996b; Truesdale and Jones, 1996; Baker et al., 2001; Hou et al., 2009), aerosols (Gilfedder et al., 2008; Droste et al., 2021) and snow (Gilfedder et al., 2008) in the marine boundary layer indicate that aqueous iodide and iodate coexist. Hou et al. (2009) reviewed wet iodine speciation data and reported that IO_3^- predominates over I^- from marine sources/air masses whereas I^- predominates from continental air masses.

There are several ways that I^- (or reduced I) can form in rainwater and aerosols. The interconversion between IO_3^- and I^- at the pH of wet deposition also leads to HOI and I_2, which can react with organic material forming C-I bonds that can release I^- (section 4.6). This material has been given the term soluble organically bound iodine and can be larger than the sum of the concentrations of IO_3^- and I^- in

aerosols (Gilfedder et al., 2008; Droste et al., 2021). Soluble organically bound iodine can form from release of natural organic iodine from land and sea (a primary source) or from the reaction of natural organic material with HOI or I_2 in the atmosphere (a secondary source). On photolysis of C-I, I• forms and reacts with O_3, and on C-I reaction with nucleophiles, I^- forms. During a study on the formation of cloud condensation nuclei, Huang et al. (2022) also showed that natural gaseous organic material in the marine boundary layer reacts with IO_3^- in aerosols resulting in gaseous I_2, which can be reoxidized to IO_3^- (catalysis) or react to form organic-I compounds. Lastly, Cuevas et al. (2022) reported that photolysis of IO_3^- particles in the stratosphere at a wavelength of about 260 nm can lead to gaseous I• and O_2 during transport from the tropics to the Antarctic region. Thus, there are several pathways for reduction of IO_3^- in the atmosphere.

5 Conclusions

The reduction of IO_3^- to I^- in solution is a facile process by biotic and abiotic reactions. The intermediates IO_2^- and HOI dictate the reactivity sequence *via* a combination of thermodynamic and kinetic considerations. The IO_3^- to IO_2^- conversion is the least favorable and likely controlling step in this reaction sequence, but there is no need for nitrate reductase for IO_3^- reduction based on numerous studies. The data from this study indicate that once IO_2^- forms there is no thermodynamic barrier to I^- formation. Chemical reduction of all iodine species (not iodide) by sulfide, Fe^{2+} and Mn^{2+} are favorable at seawater and sedimentary pH values, but only sulfide has been studied in the laboratory at oceanic pH values. Dissimilatory IO_3^- reduction during organic matter decomposition seems to be a key process as the IO_3^-/IO_2^- couple is more favorable than the NO_3^-/NO_2^- couple.

However, the oxidation of I^- back to IO_3^- *via* $^3O_2$ has a major thermodynamic barrier in solution, and the disproportionation of HOI at seawater pH values is not measurable. Thus, ROS, oxidized Mn and microbes are important for I^- oxidation to IO_3^- due to favorable thermodynamics and kinetics (Table 2). Recent reports of microbial oxidation have not documented the entire six-electron oxidation in a stepwise manner so further work on this topic is necessary. Oxidation of I^- by oxidized Mn is a pH dependent reaction and less likely at seawater pH values but could occur in sedimentary environments. The reactions of O_3 and •OH with iodine species (not IO_3^-) are thermodynamically favorable over all pH. However, ROS are not normally in significant concentration in seawater to influence IO_3^- formation. Notable exceptions are for (1) sea surface microlayer, which adsorbs atmospheric O_3, and (2) the reaction of Fe^{2+} with O_2 that leads to Fenton chemistry with •OH production. Systems where Fenton chemistry can occur are at/near hydrothermal vents (Shaw et al., 2021), submarine groundwaters (Burns et al., 2010), and sediments or water columns where O_2 and Fe^{2+} concentration profiles overlap including ancient earth (Chan et al., 2016).

I^- is a major sink for O_3 in the sea surface microlayer and the atmosphere. IO_3^- formation in the atmosphere and IO_3^- redeposition to surface seawater may be major iodine processes with the latter being similar to the deposition of trace metals from wet and dry deposition to the surface ocean (e.g., Chance et al., 2015; Meskhidze et al., 2019). Most atmospheric iodine originates from marine sources where I^- oxidation to I_2 and homolytic cleavage of C-I bonds occurs; thus, gaseous iodine emissions from the ocean are reduced. IO_3^- forms from these sources during oxidation by O_3 in the atmosphere. An estimate of atmospheric deposition of IO_3^- to the ocean surface could be made by using the amount of IO_3^- in rainwater and aerosols that would be returned to the ocean surface, but more information on iodine speciation in rainwater and aerosols is needed as global spatial coverage appears limited. Despite major advances in iodine geochemistry over the last two decades, significant research is still needed on the processes that affect I^- oxidation to IO_3^- in the atmosphere, seawater and ocean sediments.

Author contributions

The author confirms being the sole contributor of this work and has approved it for publication.

Acknowledgments

The author thanks NSF for funding his group's research on iodine marine chemistry over his career, and Thomas Church and Timothy Ferdelman for suggesting the author's initial foray into iodine chemistry. The author thanks the reviewers and guest editor, Rosie Chance, for their comments and constructive suggestions to improve the manuscript.

Conflict of interest

The author declares that the research was conducted in the absence of any commercial or financial relationships that could be construed as a potential conflict of interest.

Publisher's note

References

Allard, S., and Gallard, H. (2013). Abiotic formation of methyl iodide on synthetic birnessite: A mechanistic study. *Sci. Total Environ.* 463–464, 169–175. doi: 10.1016/j.scitotenv.2013.05.079

Allard, S., von Gunten, U., Sahli, E., Nicolau, R., and Gallard, H. (2009). Oxidation of iodide and iodine on birnessite (δ-MnO2) in the pH range 4–8. *Water Res.* 43, 3417–3426. doi: 10.1016/j.watres.2009.05.018

Amachi, S. (2008). Microbial contribution to global iodine cycling: volatilization, accumulation, reduction, oxidation, and sorption of iodine. *Microbes Environ.* 23 (4), 269–276. doi: 10.1264/jsme2.me08548

Amachi, S., and Iino, T. (2022). The genus *Iodidimonas*: From its discovery to potential applications. *Microorganisms* 10, 1661. doi: 10.3390/microorganisms10081661

Amachi, S., Kawaguchi, N., Muramatsu, Y., Tsuchiya, S., Watanabe, Y., Shinoyama, H., et al. (2007). Dissimilatory iodate reduction by marine pseudomonas sp. strain SCT. *Appl. Environ. Microbiol.* 73, 5725–5730. doi: 10.1128/AEM.00241-07

Anschutz, P., Sundby, B., Lefrançois, L., Luther, III, G. W., and Mucci, A. (2000). Interactions between metal oxides and species of nitrogen and iodine in bioturbated marine sediments, geochim. *Cosmochim. Acta* 64, 2751–2763. doi: 10.1016/S0016-7037(00)00400-2

Baker, A. R., Tunnicliffe, C., and Jickells, T. D. (2001). Iodine speciation and deposition fluxes from the marine atmosphere. *J. Geophys. Res.* 106, 28743–28749. doi: 10.1029/2000JD000004

Bard, A. J., Parsons, R., and Jordan, J. (1985). *Standard potentials in aqueous solution. 1st ed* (New York: M. Dekker), 834.

Bielski, B. H. J., Cabelli, D. E., Arudi, R. L., and Ross, A. B. (1985). Reactivity of HO_2/O_2^- radicals in aqueous solution. *J. Phys. Chem. Ref. Data* 14, 1041–1100. doi: 10.1063/1.555739

Bluhm, K., Croot, P., Wuttig, K., and Lochte, K. (2010). Transformation of iodate to iodide in marine phytoplankton driven by cell senescence. *Aquat. Biol.* 11, 1–15. doi: 10.3354/ab00284

Burns, J. M., Craig, P. S., Shaw, T. J., and Ferry, J. L. (2010). Multivariate examination of Fe(II)/Fe(III) cycling and consequent hydroxyl radical generation. *Environ. Sci. Technol.* 44, 7226–7231. doi: 10.1021/es903519m

Butler, A., and Sandy, M. (2009). Mechanistic considerations of halogenating enzymes. *Nature* 460, 848–854. doi: 10.1038/nature08303

Buxton, G. V., Greenstock, C. L., Helman, W. P., and Ross, A. B. (1988). Critical review of rate constants for reactions of hydrated electrons, hydrogen atoms and hydroxyl radicals in aqueous solution. *J. Phys. Chem. Ref. Data* 17, 513–886. doi: 10.1063/1.555805

Campos, M., Farrenkopf, A., Jickells, T., and Luther, G. (1996). A comparison of dissolved iodine cycling at the Bermuda Atlantic time-series station and Hawaii ocean time-series station. *Deep-Sea Res. II Top. Stud. Oceanogr.* 43 (2), 455–466. doi: 10.1016/0967-0645(95)00100-X

Campos, M. L. A. M., Nightingale, P. D., and Jickells, T. D. (1996). A comparison of methyl iodide emissions from seawater and wet depositional fluxes of iodine over the southern north Sea. *Tellus* 48, 106–114. doi: 10.3402/tellusb.v48i1.15830

Carpenter, L. J., Chance, R. J., Sherwen, T., Adams, T. J., Ball, S. M., Evans, M. J., et al. (2021). Marine iodine emissions in a changing world. *Proc. R. Soc A* 477, 20200824. doi: 10.1098/rspa.2020.0824

Carpenter, L., MacDonald, S., Shaw, M., Kumar, R., Saunders, R. W., Parthipan, R., et al. (2013). Atmospheric iodine levels influenced by sea surface emissions of inorganic iodine. *Nat. Geosci.* 6, 108–111. doi: 10.1038/ngeo1687

Carrano, M. W., Yarimizu, K., Gonzales, J. L., Cruz-López, R., Edwards, M. S., Tymon, T. M., et al. (2020). The influence of marine algae on iodine speciation in the coastal ocean. *Algae* 35 (2), 167–176. doi: 10.4490/algae.2020.35.5.25

Chance, R. J., Jickells, T. D., and Baker, A. R. (2015). Atmospheric trace metal concentrations, solubility and deposition fluxes in remote marine air over the south-east Atlantic. *Mar. Chem.* 177, 45–56. doi: 10.1016/j.marchem.2015.06.028

Chance, R., Malin, G., Jickells, T., and Baker, A. R. (2007). Reduction of iodate to iodide by cold water diatom cultures. *Mar. Chem.* 105, 169–180. doi: 10.1016/j.marchem.2006.06.008

Chance, R. J., Tinel, L., Sherwen, T., Baker, A. R., Bell, T., Brindle, J., et al. (2019). Global sea-surface iodide observations 1967–2018. *Sci. Data* 6, 286. doi: 10.1038/s41597-019-0288-y

Chan, C. S., Emerson, D., and Luther, G. (2016). The role of microaerophilic fe-oxidizing micro-organisms in producing banded iron formations. *Geobiology* 14, 509–528. doi: 10.1111/gbi.12192

Colin, C., Leblanc, C., Wagner, E., Delage, L., Leize-Wagner, E., van Dorsselaer, A., et al. (2003). The brown algal kelp laminaria digitata features distinct bromoperoxidase and iodoperoxidase activities. *J. Biol. Chem.* 278, 23545–23552. doi: 10.1074/jbc.M300247200

Councell, T. B., Landa, E. R., and Lovely, D. R. (1997). Microbial reduction of iodate. *Water Air Soil pollut.* 100, 99–106. doi: 10.1023/A:1018370423790

Cuevas, C. A., Fernandez, R. P., Kinnison, D. E., Li, Q., Lamarques, J.-F., Trabelsi, T., et al. (2022). The influence of iodine on the Antarctic stratospheric ozone hole. *Proc. Natl. Acad. Sci. U.S.A.* 119, No. 7, e2110864119. doi: 10.1073/pnas.2110864119

Cutter, G. A., Moffett, J. G., Nielsdottir, M. C., and Sanial, V. (2018). Multiple oxidation state trace elements in suboxic waters off Peru: *in situ* redox processes and advective/diffusive horizontal transport. *Mar. Chem.* 201, 77–89. doi: 10.1016/j.marchem.2018.01.003

Damgaard, L. R., Jelly, C., Casciotti, K., Ward, B. B., and Revsbech, N. P. (2020). Amperometric sensor for nanomolar nitrous oxide analysis. *Anal. Chim. Acta* 1101, 135–140. doi: 10.1016/j.aca.2019.12.019

de la Cuesta, J. L., and Manley, S. L. (2009). Iodine assimilation by marine diatoms and other phytoplankton in nitrate-replete conditions. *Limnology Oceanogr.* 54, 1653–1664. doi: 10.4319/lo.2009.54.5.1653

Droste, E. S., Baker, A. R., Yodle, C., Smith, A., and Ganzeveld, L. (2021). Soluble iodine speciation in marine aerosols across the Indian and pacific ocean basins. *Front. Mar. Sci.* 8, 788105. doi: 10.3389/fmars.2021.788105

Elderfield, H., and Truesdale, V. W. (1980). On the biophilic nature of iodine in seawater. *Earth Planet. Sci. Lett.* 50, 105–114. doi: 10.1016/0012-821X(80)90122-3

Estes, E. R., Berti, D., Findlay, A. J., Hochella, M. F.Jr., Shaw, T. J., Yücel, M., et al. (2022). Differential behavior of metal sulfides in hydrothermal plumes and diffuse flows. *ACS Earth Space Chem.* 6, 1429–1442. doi: 10.1021/acsearthspacechem.1c00377

Farrenkopf, A. M., Dollhopf, M. E., Chadhain, S. N., Luther, G. W., and Nealson, K. H. (1997). Reduction of iodate in seawater during Arabian Sea shipboard incubations and in laboratory cultures of the marine bacterium *Shewanella putrefaciens* strain MR-4. *Mar. Chem.* 57 (3), 347–354. doi: 10.1016/S0304-4203(97)00039-X

Farrenkopf, A. M., and Luther, G. W. (2002). Iodine chemistry reflects productivity and denitrification in the Arabian Sea: Evidence for flux of dissolved species from sediments of western India into the OMZ. *Deep-Sea Res. II Top. Stud. Oceanogr* 49 (12), 2303–2318. doi: 10.1016/S0967-0645(02)00038-3

Finkenzeller, H., Iyer, S., He, X. C., Simon, M., Koenig, T. K., Lee, C. F., et al. (2022). The gas-phase formation mechanism of iodic acid as an atmospheric aerosol source. *Nat. Chem* 15, 129-135. doi: 10.1038/s41557-022-01067-z

Fox, P. M., Davis, J. A., and Luther, III, G. W. (2009). The kinetics of iodide oxidation by the manganese oxide mineral birnessite. *Geochim. Cosmochim. Acta* 73, 2850–2861. doi: 10.1016/j.gca.2009.02.016

Freing, A., Wallace, D. W. R., and Bange, H. W. (2012). Global oceanic production of nitrous oxide. *Phil. Trans. R. Soc B* 367, 1245–1255. doi: 10.1098/rstb.2011.0360

Gilfedder, B. S., Lai, S. C., Petri, M., Biester, H., and Hoffmann, T. (2008). Iodine speciation in rain, snow and aerosols. *Atmos. Chem. Phys.* 8, 6069–6084. doi: 10.5194/acp-8-6069-2008

Guo, J., Jiang, J., Peng, Z., Zhong, Y., Jiang, Y., Jiang, Z., et al. (2022). Global occurrence of the bacteria with capability for extracellular reduction of iodate. *Front. Microbiol.* 13. doi: 10.3389/fmicb.2022.1070601

Hardisty, D. H., Horner, T. J., Evans, Z. C., Moriyasu, R., Babbin, A. R., Wankel, S. D., et al. (2021). Limited in situ iodate reduction within the Eastern tropical north pacific oxygen deficient zone. *Earth Planetary Sci. Lett.* 554, 116676. doi: 10.1016/j.chemgeo.2019.119360

Hardisty, D. H., Horner, T. J., Wankel, S. D., Blusztajn, J., and Nielsen, S. G. (2020). Experimental observations of marine iodide oxidation using a novel sparge interface MC-ICP-MS technique. *Chem. Geol.* 532, 119360. doi: 10.1016/j.chemgeo.2019.119360

Harvey, G. R. (1980). A study of the chemistry of iodine and bromine in marine sediments. *Mar. Chem.* 8, 327–332. doi: 10.1016/0304-4203(80)90021-3

He, X.-C., Tham, Y. J., Dada, L., Wang, M., Finkenzeller, H., Stolzenberg, D., et al. (2021). Role of iodine oxoacids in atmospheric aerosol nucleation. *Science* 371, 589–595. doi: 10.1126/science.abe0298

Hepach, H., Hughes, C., Hogg, K., Collings, S., and Chance, R. (2020). Senescence as the main driver of iodide release from a diverse range of marine phytoplankton. *Biogeosciences* 17, 2453–2471. doi: 10.5194/bg-17-2453-2020

Hou, X. L., Aldahan, A., Nielsen, S. P., and Possnert, G. (2009). Time series of I-129 and I-127 speciation in precipitation from Denmark. *Environ. Sci. Technol.* 43, 6522–6528. doi: 10.1021/es9012678

Huang, R.-J., Hoffmann, T., Ovadnevaite, J., Laaksonen, A., Kokkola, H., Xu, W., et al. (2022). Heterogeneous iodine-organic chemistry fast-tracks marine new particle formation. *Proc. Natl. Acad. Sci. U.S.A.* 119, e2201729119. doi: 10.1073/pnas.2201729119

Hughes, C., Barton, E., Hepach, H., Chance, R., Pickering, M. D., Hogg, K., et al. (2021). Oxidation of iodide to iodate by cultures of marine ammonia-oxidising bacteria. *Mar. Chem.* 234, 104000. doi: 10.1016/j.marchem.2021.104000

Hung, C.-C., Wong, G. T. F., and Dunstan, W. M. (2005). Iodate reduction activity in nitrate reductase extracts from marine phytoplankton. *Bul. Mar. Sci.* 76, 61–72.

Kaltsoyannis, N., and Plane, J. M. C. (2008). Quantum chemical calculations on a selection of iodine-containing species (IO, OIO, INO_3, $(IO)_2$, $I2O_3$, $I2O_4$ and $I2O_5$) of importance in the atmosphere. *Phys. Chem. Chem. Phys.* 10, 1723–1733. doi: 10.1039/b715687c

Kennedy, H. A., and Elderfield, H. (1987a). Iodine diagenesis in pelagic deep-sea sediments. *Geochim. Cosmchim. Acta* 51, 2489–2504. doi: 10.1016/0016-7037(87)90300-0

Kennedy, H. A., and Elderfield, H. (1987b). Iodine diagenesis in non-pelagic deep-sea sediments. *Geochim. Cosmchim. Acta* 51, 2505–2514. doi: 10.1016/0016-7037(87)90301-2

Kim, K., Ju, J., Kim, B., Chung, H. Y., Vetráková, L., Heger, D., et al. (2019). Nitrite-induced activation of iodate into molecular iodine in frozen solution. *Environ. Sci. Technol.* 53, 4892–4900. doi: 10.1021/acs.est.8b06638

Koenig, T. K., Baidar, S., Campuzano-Jost, P., Cuevas, C. A., Dix, B., Fernandez, R. P., et al. (2020). Quantitative detection of iodine in the stratosphere. *Proc. Natl. Acad. Sci. U.S.A.* 117, 1860–1866. doi: 10.1073/pnas.1916828117

Küpper, F. C., Carpenter, L. J., McFiggans, G. B., Palmer, C. J., Waite, T. J., Boneberg, E.-M., et al. (2008). Iodide accumulation provides kelp with an inorganic antioxidant impacting atmospheric chemistry. *Proc. Natl. Acad. Sci. U. S. A.* 105, 6954–6958. doi: 10.1073/pnas.0709959105

Küpper, F. C., Feiters, M. C., Olofsson, B., Kaiho, T., Yanagida, S., Zimmermann, M. B., et al. (2011). Commemorating two centuries of iodine research: An interdisciplinary overview of current research. *Angewandte Chemie Int. Editions* 50, 11598–11620. doi: 10.1002/anie.201100028

Lehner, P., Larndorfer, C., Garcia-Robledo, E., Larsen, M., Borisov, S. M., Revsbech, N.-P., et al. (2015). LUMOS - a sensitive and reliable optode system for measuring dissolved oxygen in the nanomolar range. *PloS One* 10 (6), e0128125. doi: 10.1371/journal.pone.0128125

Lewis, B. L., and Luther, III, G. W. (2000). Processes controlling the distribution and cycling of manganese in the oxygen minimum zone of the Arabian Sea. *Deep Sea Res.* 47, 1541–1561. doi: 10.1016/S0967-0645(99)00153-8

Li, H.-P., Daniel, B., Creeley, D., Grandbois, R., Zhang, S., Xu, C., et al. (2014). Superoxide production by a manganese-oxidizing bacterium facilitates iodide oxidation. *Appl. Environ. Microbio* 80, 2693–2699. doi: 10.1128/AEM.00400-14

Liu, Q., Schurter, L. M., Muller, C. E., Aloisio, S., Francisco, J. S., and Margerum, D. W. (2001). Kinetics and mechanisms of aqueous ozone reactions with bromide, sulfite, hydrogen sulfite, iodide, and nitrite ions. *Inorg. Chem.* 40, 4436–4442. doi: 10.1021/ic000919j

Li, H.-P., Yeager, C. M., Brinkmeyer, R., Zhang, S., Ho, Y.-F., Xu, C., et al. (2012). Bacterial production of organic acids enhances H_2O_2-dependent iodide oxidation. *Environ. Sci. Technol.* 46, 4837–4844. doi: 10.1021/es203683v

Luther, III, G. W. (2010). The role of one and two electron transfer reactions in forming thermodynamically unstable intermediates as barriers in multi-electron redox reactions. *Aquat. Geochem.* 16, 395–420. doi: 10.1007/s10498-009-9082-3

Luther, III, G. W. (2011). Thermodynamic redox calculations for one and two electron transfer steps: Implications for halide oxidation and halogen environmental cycling. In *Aquatic Redox Chemistry* editors, P. G. Tratnyek, T. J. Grundl and S. B. Haderlein (Washington, D.C.: American Chemical Society) 15–35. doi: 10.1021/.bk-2011-1071.ch002

Luther, III, G. W. (2016). *Inorganic chemistry for geochemistry and environmental sciences: Fundamentals and applications*. (Chichester, West Sussex: John Wiley & Sons Ltd.) 456.

Luther, G. W., and Campbell, T. (1991). Iodine speciation in the water column of the black Sea. *Deep Sea Res. Part A. Oceanographic Res. Papers* 38, S875–S882. doi: 10.1007/978-94-011-2608-3_11

Luther, G. W.III, Karolewski, J. S., Sutherland, K. M., Hansel, C. M., and Wankel, S. D. (2021). The abiotic nitrite oxidation by ligand-bound manganese (III): the chemical mechanism. *Aquat. Geochem.* 27, 207–220. doi: 10.1007/s10498-021-09396-0

Luther, III, G. W., and Popp, J. I. (2002). Kinetics of the abiotic reduction of polymeric manganese dioxide by nitrite: An anaerobic nitrification reaction. *Aquat. Geochem.* 8, 15–36. doi: 10.1023/A:1020325604920

Luther, III, G. W., Wu, J., and Cullen, J. (1995). "Redox chemistry of iodine in seawater: frontier molecular orbital theory considerations," in *Aquatic chemistry: Interfacial and interspecies processes*, vol. 244 . Eds. C. P. Huang, C. R. O'Melia and J. J. Morgan (Washington, DC: American Chemical Society), 135–155. doi: 10.1021/ba-1995-0244.ch006

Martín, J. C. G., Lewis, T. R., James, A. D., Saiz-Lopez, A., and Plane, J. M. C. (2022). Insights into the chemistry of iodine new particle formation: The role of iodine oxides and the source of iodic acid. *J. Am. Chem. Soc* 144, 9240–9253. doi: 10.1021/jacs.1c12957

Meskhidze, N., Völker, C., Al-Abadleh, H. A., Barbeau, K., Bressac, M., Buck, C., et al. (2019). Perspective on identifying and characterizing the processes controlling iron speciation and residence time at the atmosphere-ocean interface mar. *Chem.* 217, 103704. doi: 10.1016/j.marchem.2019.103704

Moffett, J. W., and German, C. R. (2020). Distribution of iron in the Western Indian ocean and the Eastern tropical south pacific: An inter-basin comparison. *Chem. Geol.* 532, 119334. doi: 10.1016/j.chemgeo.2019.119334

Mohammed, A., and Liebhafsky, H. A. (1934). The kinetics of the reduction of hydrogen peroxide by the halides. *J. Amer. Chem. Soc* 56, 1680–1685. doi: 10.1021/ja01323a009

Mok, J. K., Toporek, Y. L., Hyun-Dong, S., Lee, B. D., Lee, M. H., and DiChristina, T. J. (2018). Iodate reduction by shewanella oneidensis does not involve nitrate reductase. *Geomicrobiol. J* 35, 570-579. doi: 10.1080/01490451.2018.1430189

Mopper, K., and Zhou, X. (1990). Hydroxyl radical photoproduction in the sea and its potential impact on marine processes. *Science* 250, 661–664. doi: 10.1126/science.250.4981.661

Müller, E., von Gunten, U., Bouchet, S., Droz, B., and Winkel, L. H. E. (2021). Reaction of DMS and HOBr as a sink for marine DMS and an inhibitor of bromoform formation. *Environ. Sci. Technol.* 55, 5547–5558. doi: 10.1021/acs.est.0c08189

Oldham, V. E., Jones, M. R., Siebecker, M., Mucci, A., Tebo, B. M., and Luther, III, G. W. (2019). The speciation and mobility of Mn and fe in estuarine sediments. *Aquat. Geochemistry* 25, 3–26. doi: 10.1007/s10498-019-09351-0

Ooki, A., Minamikawa, K., Meng, F., Miyashita, N., Hirawake, T., Ueno, H., et al. (2022). Marine sediment as a likely source of methyl and ethyl iodides in subpolar and polar seas. *Commun. Earth Environ.* 3, 180. doi: 10.1038/s43247-022-00513-7

Owings, S. M., Laurie Bréthous, L., Eitel, E. M., Fields, B. P., Boever, A., Beckler, J. S., et al. (2021). Differential manganese and iron recycling and transport in continental margin sediments of the northern gulf of Mexico. *Mar. Chem.* 229, 103908. doi: 10.1016/j.marchem.2020.103908

Powers, L. C., and Miller, W. L. (2014). Blending remote sensing data products to estimate photochemical production of hydrogen peroxide and superoxide in the surface ocean. *Environ. Sci. Process. Impacts* 16, 792–806. doi: 10.1039/C3EM00617D

Revsbech, N. P., Larsen, L. H., Gundersen, J., Dalsgaard, T., Ulloa, O., and Thamdrup, B. (2009). Determination of ultra-low oxygen concentrations in oxygen minimum zones by the STOX sensor. *Limnol. Oceanogr. Methods* 7, 371–381. doi: 10.4319/lom.2009.7.371

Reyes-Umana, V., Henning, Z., Lee, K., Barnum, T. P., and Coates, J. D. (2022). Genetic and phylogenetic analysis of dissimilatory iodate-reducing bacteria identifies potential niches across the world's oceans. *ISME J.* 16, 38–49. doi: 10.1038/s41396-021-01034-5

Rickard, D., and Luther, III, G. W. (2007). Chemistry of iron sulfides. *Chem. Rev.* 107, 514–562. doi: 10.1021/cr0503658

Rue, E. L., Smith, G. J., Cutter, G. A., and Bruland, K. W. (1997). The response of trace element redox couples to suboxic conditions in the water column. deep-Sea res. *I Oceanogr. Res. Pap.* 44 (1), 113–134. doi: 10.1016/S0967-0637(96)00088-X

Schmitz, G. (2008). Inorganic reactions of Iodine(III) in acidic solutions and free energy of iodous acid formation. *Int. J. Chem. Kinet.* 40, 647–652. doi: 10.1002/kin.20344

Schwarz, H. A., and Bielski, B. H. J. (1986). Reactions of HO_2 and $O2^-$ with iodine and bromine and the I_2^- and I atom reduction potentials. *J. Phys. Chem.* 90, 1445–1448. doi: 10.1021/j100398a045

Shaw, T. J., Luther, G. W.III, Rosas, R., Oldham, V. E., Coffey, N. R., Ferry, J. L., et al. (2021). Fe-catalyzed sulfide oxidation in hydrothermal plumes is a source of reactive oxygen species to the ocean. *Proc. Natl. Acad. Sci. U.S.A.* 118 (40), e2026654118. doi: 10.1073/pnas.2026654118

Shimmield, G. B., and Pedersen, T. F. (1990). The geochemistry of reactive trace metals and halogens in hemipelagic continental margin sediments. *Rev. Aquat. Sci.* 3, 255–279.

Shin, H.-D., Toporek, Y., Mok, J. K., Maekawa, R., Lee, B. D., Howard, M. H., et al. (2022). Iodate reduction by *Shewanella oneidensis* requires genes encoding an extracellular dimethylsulfoxide reductase. *Front. Microbiol.* 13. doi: 10.3389/fmicb.2022.852942

Sipilä, M., Sarnela, N., Jokinen, T., Henschel, H., Junninen, H, Kontkanen, J., et al. (2016). Molecular-scale evidence of aerosol particle formation *via* sequential addition of HIO_3. *Nature* 537, 532–534. doi: 10.1038/nature19314

Stanbury, D. (1989). "Reduction potentials involving inorganic free radicals in aqueous solution," in *Advances in inorganic chemistry*, vol. 33 . Ed. A. G. Sykes (New York: Academic Press), 69–138.

Stumm, W., and Morgan, J. J. (1996). *Aquatic chemistry. 3rd edition* (New York: John Wiley), 1022.

Sunday, M. O., Takeda, K., and Sakugawa, H. (2020). Singlet oxygen photogeneration in coastal seawater: Prospect of Large-scale modeling in seawater surface and its environmental significance. *Environ. Sci. Technol.* 54, 6125–6133. doi: 10.1021/acs.est.0c00463

Sutherland, K. M., Wankel, S. D., and Hansel, C. M. (2020). Dark biological superoxide production as a significant flux and sink of marine dissolved oxygen. *Proc. Natl. Acad. Sci. U.S.A.* 117, 3433–3439. doi: 10.1073/pnas.1912313117

Szlamkowicz, I. B., Fentress, A. J., Longen, L. F., Stanberry, J. S., and Anagnostopoulos, V. A. (2022). Transformations and speciation of iodine in the environment as a result of oxidation by manganese minerals. *ACS Earth Space Chem.* 6, 1948–1956. doi: 10.1021/acsearthspacechem.1c00372

Teiwes, R., Elm, J., Bilde, M., and Pedersen, H. B. (2019). The reaction of hydrated iodide $I(H_2O)^-$ with ozone: A new route to IO_2^- products. *Phys. Chem. Chem. Phys.* 21, 17546–17554. doi: 10.1039/C9CP01734H

Trouwborst, R. E., Clement, B. G., Tebo, B. M., Glazer, B. T., and Luther, G. W.III (2006). Soluble Mn(III) in suboxic zones. *Science* 313, 1955–1957. doi: 10.1126/science.1132876

Truesdale, V. W., and Jones, S. D. (1996). The variation of iodate and total iodine in some UK rainwaters during 1980-1981. *J. Hydrology* 179, 67–86. doi: 10.1016/0022-1694(95)02873-0

Truesdale, V. W., and Luther, III, G. W. (1995). Molecular iodine reduction by natural and model organic substances in seawater. *Aquat. Geochem.* 1, 89–104. doi: 10.1007/BF01025232

Truesdale, V. W., Watts, S. F., and Rendell, A. (2001). On the possibility of iodide oxidation in the near-surface of the black Sea and its implications to iodine in the general ocean. *Deep-Sea Res. I Oceanogr. Res. Pap* 48 (11), 2397–2412. doi: 10.1016/S0967-0637(01)00021-8

Waite, T. J., and Truesdale, V. W. (2003). Iodate reduction by *Isochrysis galbana* is relatively insensitive to de-activation of nitrate reductase activity–are phytoplankton really responsible for iodate reduction in seawater? *Mar. Chem.* 81, 137–148.

Weiss, R. F., and Price, B. A. (1980). Nitrous oxide solubility in water and seawater. *Mar Chem.* 8, 347–359. doi: 10.1016/0304-4203(80)90024-9

Whalley, L. K., Furneaux, K. L., Goddard, A., Lee, J. D., Mahajan, A., Oetjen, H., et al. (2010). The chemistry of OH and HO_2 radicals in the boundary layer over the tropical Atlantic ocean. *Atmos. Chem. Phys.* 10, 1555–1576. doi: 10.5194/acp-10-1555-2010

Wilkinson, F., Helman, W. P., and Ross, A. B. (1995). Rate constants for the decay and reactions of the lowest electronically excited singlet state of molecular oxygen in solution. *expanded revised compilation. J. Phys. Chem. Ref. Data* 24, 663–1021. doi: 10.1063/1.555965

Wong, G. T. F. (1991). The marine geochemistry of iodine. *Rev. Aquat. Sci.* 4, 45–73.

Wong, G. T. F. (2001). Coupling iodine speciation to primary, regenerated or "new" production: A re-evaluation. *Deep Sea Res. Part I Oceanographic Res. Papers* 48, 1459–1476. doi: 10.1016/S0967-0637(00)00097-2

Wong, G. T., and Brewer, P. G. (1977). The marine chemistry of iodine in anoxic basins. *Geochim. Cosmochim. Acta* 41 (1), 151–159. doi: 10.1016/0016-7037(77)90195-8

Wong, G. T. F., Piumsomboon, A. U., and Dunstan, W. M. (2002). The transformation of iodate to iodide in marine phytoplankton cultures. *Mar. Ecol. Prog. Ser.* 237, 27–39. doi: 10.3354/meps237027

Wong, G. T., Takayanagi, K., and Todd, J. T. (1985). Dissolved iodine in waters overlying and in the orca basin, gulf of Mexico. *Mar. Chem.* 17, 177–183. doi: 10.1016/0304-4203(85)90072-6

Wong, G. T., and Zhang, L.-S. (2008). The kinetics of the reactions between iodide and hydrogen peroxide in seawater. *Mar. Chem.* 111, 22–29. doi: 10.1016/j.marchem.2007.04.007

Yamazaki, C., Kashiwa, S., Horiuchi, A., Kasahara, Y., Yamamura, S., and Amachi, S. A. (2020). Novel dimethylsulfoxide reductase family of molybdenum enzyme. *Environ. Microbiol.* 22, 2196–2212. doi: 10.1111/1462-2920.14988

Yuan, J., and Shiller, A. M. (2001). The distribution of hydrogen peroxide in the southern and central Atlantic ocean. *Deep Sea Res. Part II Top. Stud. Oceanogr* 48, 2947–2970. doi: 10.1016/S0967-0645(01)00026-1

Zhang, J.-Z., and Whitfield, M. (1986). Kinetics of inorganic reactions in seawater. 1. the reduction of iodate by bisulphide. *Mar. Chem.* 19, 121–137. doi: 10.1016/0304-4203(86)90044-7

Žic, V., and Branica, M. (2006). The distributions of iodate and iodide in rogoznica lake (East Adriatic coast). *Estuar. Coast. Shelf Sci.* 66 (1), 55–66. doi: 10.1016/j.ecss.2005.07.022

Žic, V., Truesdale, V. W., and Cukrov, N. (2008). The distribution of iodide and iodate in anchialine cave waters–evidence for sustained localised oxidation of iodide to iodate in marine water. *Mar. Chem.* 112 (3–4), 168–178. doi: 10.1016/j.marchem.2008.09.001